1-1-2003

# A study of PEM fuel cell modeling

Peng Quan
*Ryerson University*

# A STUDY OF PEM FUEL CELL MODELING

by

Peng Quan

A Project Report Submitted

in

Partial Fulfillment of the Requirements for the Degree of

MASTER OF ENGINEERING

in the Department of Mechanical and Industrial Engineering

© Peng Quan, 2003

Ryerson University

UMI Number: EC52893

INFORMATION TO USERS

The quality of this reproduction is dependent upon the quality of the copy submitted. Broken or indistinct print, colored or poor quality illustrations and photographs, print bleed-through, substandard margins, and improper alignment can adversely affect reproduction.

In the unlikely event that the author did not send a complete manuscript and there are missing pages, these will be noted. Also, if unauthorized copyright material had to be removed, a note will indicate the deletion.

# UMI®

Supervisor: Dr. Jun Cao

# Abstract

Fuel cells are electrochemical devices that directly convert the chemical energy of reaction of a fuel and an oxidant (usually hydrogen and oxygen) into electricity. Detailed measurements of properties such as the fluid flow distribution, species concentration, temperature distribution and local current densities are difficult to obtain during the operation of a fuel cell. Nonetheless, information like that is critical for improving the fuel cell performance, reducing cost and identifying possible failure mechanisms. Therefore, numerical models that are capable of producing this information would be very useful for design and optimization as well as improved fundamental understanding of transport processes in fuel cells.

In this project a two-dimensional, non-isothermal and non-isobaric computational model of a PEM fuel cell is formulated. The model is coupled with a computational fluid dynamics model for diffusive transport in the electrodes and convective transport in the gas flow channel, which is built principally upon the conservation laws for mass, momentum and energy. Then the following four phenomenological equations are also involved: the *Stefan-Maxwell* equation for the description of multi-species diffusion; the *Bulter-Volmer* equation for the description of first-order reaction kinetics; the *Nernst-Planker* equation for the description of proton flux through membrane; and the *Schlögl* equation for the description of water velocity in membrane. The focus of the project is placed on the study of partial hydration in the membrane. For this propose, we develop our membrane model partly based on empirical relationships to account explicitly for water diffusion, pressure distribution and electro-osmotic drag; meanwhile,

thermal effects are introduced implicitly via the variation of membrane transport parameters as functions of temperature.

Although the solution of the present model is beyond the scope of the project, we are trying to embed the general solution ideas in our modeling work by giving, for all computation domains, detailed boundary conditions and corresponding properties and parameters that are critical for the prediction accuracy of the model.

# Table of Contents

v

# List of Tables

# List of Figures

# Nomenclature

| Symbol | Description | Unit |
|---|---|---|
| $a$ | Chemical activity | - |
| $c$ | Concentration | $mol/m^3$ |
| $c_p$ | Specific heat capacity at constant pressure | $J/(kg°C)$ |
| $D$ | Diffusion coefficient | $m^2/s$ |
| $E$ | Cell potential | V |
| $E_m$ | Equivalent membrane weight | $kg/mol$ |
| $e$ | Membrane constant | $mol/m^3$ |
| $F$ | Faraday constant | 96487 Coulomb/mol |
| $f$ | Swelling constant coefficient | - |
| $\bar{g}$ | Specific Gibb's free energy | $J/mol$ |
| $H$ | Total specific enthalpy | $J/mol$ |
| $\bar{h}$ | Specific enthalpy | $J/mol$ |
| $i$ | Current density | $A/m^2$ |
| $i_0$ | Exchange current density | $A/m^2$ |
| $K$ | Chemical equilibrium constant | - |
| $k_\phi$ | Electric permeability | $m^2$ |
| $k_p$ | Hydraulic permeability | $m^2$ |
| $M$ | Molecular weight | $kg/mol$ |

| Symbol | Description | Unit |
| --- | --- | --- |
| $\vec{N}$ | Molar flux | mol/ (m²s) |
| $n$ | Molar number of electrons transferred | - |
| $n_d$ | Electro-osmotic drag coefficient | - |
| $p$ | Pressure | Pa |
| $\dot{Q}$ | Heat flux | W/m² |
| $\dot{q}_r$ | Heat source (flux) | W/m² |
| $R$ | Universal gas constant | 8.3145 J/(mol·K) |
| $S$ | Mass source/sink | kg/(m³-s) |
| $\bar{s}$ | Specific entropy | J/(mol·K) |
| $T$ | Temperature | K |
| $\vec{U}$ | Velocity vector | m/s |
| $\vec{U}_i$ | Diffusion velocity of species $i$ | m/s |
| $\vec{u}_i$ | Absolute velocity of species $i$ | m/s |
| $u$ | X - component of $\vec{U}$ | m/s |
| $v$ | Y - component of $\vec{U}$ | m/s |
| $V$ | Electrical potential | V |
| $\dot{W}$ | Work rate | W/ m² |
| $X$ | Molar fraction | - |
| $x$ | Average molar concentration | mol/m³ |
| $Z$ | Charge number | - |

| Greek Symbols | Description | Unit |
|---|---|---|
| $\phi$ | Electrical potential inside the membrane | V |
| $\alpha$ | Relative humidity | - |
| $\beta$ | Transfer coefficient | - |
| $\gamma$ | Concentration coefficient | - |
| $\varepsilon$ | Efficiency | - |
| $\varepsilon_w^m$ | Volume fraction of water in membrane | - |
| $\gamma_g$ | Electrode porosity | - |
| $\varsigma$ | Stoichiometric flow ratio | - |
| $\xi$ | Dilatational viscosity | kg/(m-s) |
| $\eta$ | Activation overpotential | V |
| $\kappa$ | Membrane conductivity | $1/(\Omega \cdot m)$ |
| $\Gamma$ | Molecular diffusion coefficient | kg/(m-s) |
| $\lambda$ | Thermal conductivity | W/(m-K) |
| $\lambda$ | Water content (Chapter 6 only) | - |
| $\mu$ | Viscosity | kg/(m-s) |
| $\vartheta$ | Fuel utilization coefficient | - |
| $\omega$ | Mass fraction | - |
| $\rho$ | Density | kg/m$^3$ |
| $\rho_m^{dry}$ | Dry membrane density | kg/m$^3$ |
| $\sigma$ | Surface tension | N/m$^2$ |

| Super/subscripts | Description |
| --- | --- |
| $()^0$ | Standard state |
| $()'$ | Transpose |
| $()^{eff}$ | Effective |
| $()^{sat}$ | Saturated |
| $()^{ref}$ | Reference |
| $()_{out}$ | Outflow |
| $()_{in}$ | Inflow |
| $()_{rev}$ | Reversible |
| $()_a$ | Anode |
| $()_c$ | Cathode |
| $()_p$ | Proton |
| $()_{act}$ | Activation |
| $()_{conc}$ | Concentration |
| $()_{ohm}$ | Ohmic |
| $()_e$ | Voltage |
| $()_f$ | Faradaic or fuel |
| $()_{envir}$ | Environment |
| $()_{ave}$ | Average |
| $()_l$ or $()_w$ | Liquid water |
| $()_{gr}$ | Graphite matrix |

# Acknowledgements

I am very grateful to my supervisor, Dr. Jun Cao, for giving me the opportunity to work on such an exciting project and for his constant encouragement and valuable guidance throughout this work.

Most of all, I want to thank my parents and my wife for their unconditional support throughout all the years of my education. This project would not have been possible without them.

# Chapter 1 Introduction

## 1.1 Background

Fuel Cells (FC's) are electrochemical devices that directly convert the chemical energy of fuel into electricity. Unlike battery, a fuel cell does not run down or require recharging. It will produce energy in the form of electricity and heat as long as fuel is supplied.

Fuel cells at standard working conditions can theoretically achieve an efficiency as high as 83 percent. Other advantages of fuel cells include mechanical simplicity, modularity, lower noise and, of top importance, zero emission that are directly attributable to the reduction of air pollution and greenhouse effect.

Statistics showed that nearly 30% of urban $CO_2$ emissions in OECD (Organization for Economic Co-operation and Development) countries in 1993 came from transportation, which consumed a large quantity of fossil fuel. So replacing internal combustion engines with a more efficient and environmentally benign technology is highly desirable. Amongst various types of fuel cells being developed, the Proton Exchange Membrane (PEM) fuel cell characterized by the use of a polymer electrolyte membrane appear to be the best candidate for powering

commercial and private vehicles owing to its simplicity in design and its low-temperature operating condition.

However, compared to IC engines and batteries, currently PEM fuel cells are significantly more expensive. The commercialization of PEM fuel cells requires reducing cost and increasing power density through engineering optimization, which can be implemented on the basis of a better understanding of PEM fuel cell operation mechanism. Detailed measurements of properties such as the fluid flow distribution, species concentration, temperature distribution and local current densities are difficult to obtain during the operation of a fuel cell. Nonetheless, such information is critical for improving the fuel cell performance, reducing cost and identifying possible failure mechanisms. Therefore, numerical models that are capable of producing this information would be very useful for design and optimization as well as fundamental understanding of transport processes in fuel cells.

In this project, a complete two-dimensional, non-isothermal, and non-isobaric model will be formulated for a single PEM fuel cell. In particular, water management of PEM fuel cells is a critical operation issue. Optimal operation is achieved by carefully balancing the supply and removal of water vapor to ensure that neither flooding of the electrodes nor drying out of the membrane takes place. Protonic conductivity is strongly dependent on the membrane water content, and high conductivity required for efficient operation can only be achieved by maintaining the membrane near full water saturation. The concentration of this project is to examine the effects of partial hydration in membrane during PEM fuel cell operation.

## 1.2 Operation Principle of a PEM Fuel Cell

A PEM fuel cell consists of a membrane sandwiched by two porous electrodes, along with two thin catalyst layers located at the anode-membrane and the cathode-membrane interface, respectively. Oxygen passes over one electrode and hydrogen over the other, generating electricity, water and heat.

In a contemporary PEM fuel cell, reformed hydrocarbon (main composition: $H_2$ and $CO_2$) and air (main composition: $O_2$ and $N_2$) are almost invariably adopted as fuel and oxidant, respectively.

Figure 1 shows the operation principle of a PEM Fuel Cell involving the following transport processes:
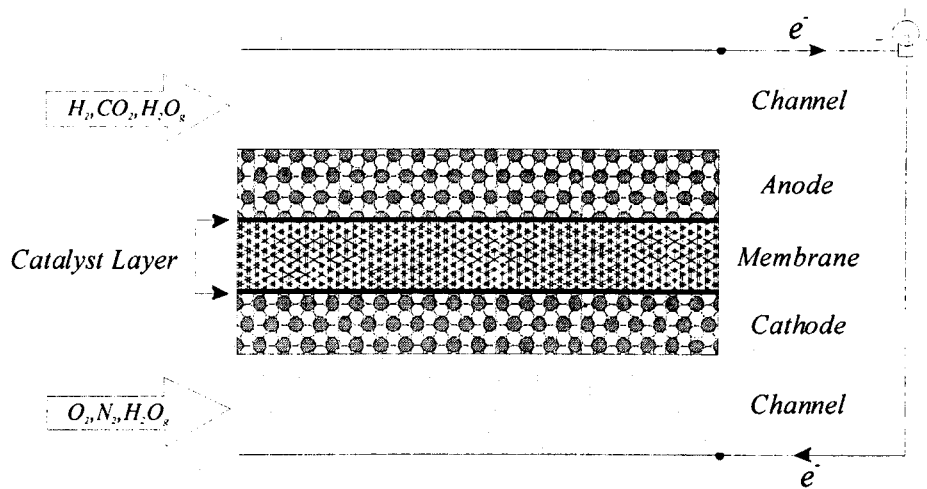


Figure 1 Operating scheme of a PEM Fuel Cell

On the anode side,

- Humidified hydrogen fuel mixture ($H_2$, $CO_2$ and $H_2O_g$) flows into the anode channel;

- Hydrogen diffuses through the porous gas-diffusion anode;

- At the anode-membrane catalyst layer the following electrochemical reaction takes place:

$$H_2 \rightarrow 2H^+ + 2e^-$$ (1.1)

- Electrons flow through the external circuit where they produce electric work; meanwhile, protons migrate through the membrane towards the cathode side;

On the cathode side, we have the following similar processes,

- Humidified air ($O_2$, $N_2$ and $H_2O_g$) enters the cathode channel;

- Oxygen diffuses through the porous gas-diffusion cathode;

- A reduction reaction producing water and heat takes place at the cathode-side catalyst layer:

$$\frac{1}{2}O_2 + 2H^+ + 2e^- \rightarrow H_2O(+Heat)$$ (1.2)
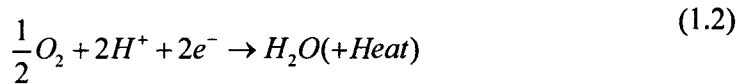
For a single PEM fuel cell, its total amount of current is related to the geometrical cell area by the current density of the cell in [A/cm$^2$]. And the product of current density and cell voltage gives the power density in [w/cm$^2$] of a single cell, which is often shown via the polarization curve.

## 1.3 Fuel Cell Components

**Proton Exchange Membrane**

One important part of a PEM fuel cell is the proton exchange membrane, a polymer electrolyte. The acidic polymeric membrane conducting protons but repelling electrons makes the electrons travel through the outer circuit providing the electric work. Membrane is characterized by the fixed-charge concentration: a higher fixed-charges concentration can lead to a higher protonic conductivity of the membrane. A commonly used electrolyte material is Nafion from DuPont, which is also the one considered in this project.

In PEM fuel cell it is particularly important to maintain appropriate water content in the electrolyte membrane, since the conductivity depends directly on water content. However, membrane saturation needs to be balanced between water removal and excessive water condensation in the gas diffusion electrodes. In this project, we describe a mathematical model for the membrane that takes into account the diffusion of water, the pressure variation, and the electro-osmotic drag in the membrane, which can be used to sophisticatedly predict the water transport fate in membrane.

**Catalyst Layer**

Although the catalyst layer is a relatively small part of the cell, it is the heart of the fuel cell energy transformation mechanism. Here the fuel and oxidant react electrochemically to produce electrical work. However, the electrochemical reactions in PEM fuel cells occur slowly especially at the cathode side. In order to enhance the electrochemical reaction rates, a

catalyst layer, which usually consists of small particles of platinum catalyst supported on larger carbon particles, is needed. These carbon particles have to be mixed with some electrolyte material in order to ensure that the protons can migrate towards the reaction site. The composition, morphology, and thickness of catalyst layer are critical in determining the performance of a cell and also the resulting cost of fuel cells.

The study conducted by Ticianelli *et al.* [1] shows that the optimum amount of Nafion loading in PEM fuel cells is 3.3% for high current densities. And the optimum value of catalyst layer thickness is found to be $10 \mu m$ [2] because almost all of the electrochemical reactions occur within a $10 \mu m$ thick layer close to the membrane.

**Gas Diffusion Electrodes**

The electrode region consists of the gas transport substrate which serves the purposes of current collection and gas transport medium. GDE's are characterized mainly by their thickness (between $100 \mu m$ and $300 \mu m$) and porosity. The assembly of the membrane and the gas-diffusion layer including the catalyst is called the Membrane-Electrode-Assembly (MEA).

**Bipolar Plates**

Separating different cells in a fuel cell stack and feeding the reactant gases to the gas-diffusion electrodes are the main duties of bipolar plates. The gas-flow channels are curved into the bipolar plates, which should otherwise be as thin as possible to reduce the weight and volume requirements. Also, maintaining a good electrical connection between the bipolar

plates and the gas-diffusion layers to minimize the contact resistance and hence ohmic losses is of importance.

## 1.4 Literature Review

In the past decade, fuel cell modeling has been used extensively to provide understanding about fuel cell performance. Although numerous researchers have focussed on different aspects of the fuel cell, the general trend from one-dimensional to multi-dimensional, from single-phase to multi-phase, from simple to complex has been established. Amongst all of these models, those addressing water-management issues are especially of interest and should be mentioned particularly in this project.

One of the earlier models addressing water management in PEM fuel cells was developed by Bernardi [3]. The primary focus of this one-dimensional model was the humidification requirements of inlet gases to maintain a state of water balance in PEM fuel cell. This work assumes that the cell is isothermal, the gas diffusion electrodes are free of water droplets, and that only water vapour is produced by the electrochemical reaction. Further assumptions are that the electro-osmotic drag of water and pressure induced flow across the membrane are insignificant next to the flow caused by a concentration gradients. These assumptions are valid for a thin membrane. Results of Bernardi's model suggest that the current density needed to maintain a water balance increases with increasing temperature due to larger water evaporation. Her work also suggests that oxygen transport in the cathode may limit fuel cell performance due to the current required to maintain water balance being higher than the diffusion-limiting

current density.

Bernardi continued her modeling work with Verbrugge by investigating the performance of a gas-fed porous cathode bonded to an ion-exchange membrane [4]. In this model, the cell is assumed to be isothermal and the gas streams ideal. The membrane is assumed to be fully hydrated; however, unlike her previous model, the flux of water through the membrane due to pressure and potential gradients is addressed. The possibility of liquid water as well as vapour flux in the electrode is considered. This model is derived from analytic expressions describing the physical processes occurring in cathode electrode, catalyst layer and membrane. The effects of hydrogen electrode are neglected. The results of this model predict a performance for a complete PEM fuel cell that agrees well with some experimental work. Results show that at higher operating currents, the resistance of the membrane is a significant contributor to overall polarization. The model also predicts that at typical operating currents, the cathode reaction is essentially a surface reaction at the front of the catalyst layer due to low reactant permeability.

Bernardi and Verbrugge completed their model evolution with a one-dimensional, isothermal model of a complete PEM MEA [5]. A good agreement with experimental cell polarization curves was achieved and the use of membranes with varying thickness was investigated. Also, the results of using a Dow membrane as compared to Nafion are explored. Experimentally determined parameters are used wherever possible; however, the cathode exchange current density per unit volume is adjusted to fit performance data. The hydraulic permeability is also adjusted to fit experimental water-transport characteristics. Besides, the results of the model shows that membrane dehydration can pose limitations on operating current density. They suggest that electrodes with low hydraulic permeability are advantageous

for maintaining membrane hydration.

Bernardi and Berbrugge's work is usually recognized as the starting point of contemporary PEM fuel cell modeling study and has been adopted as the basis for further modeling investigation by many researchers.

A significant amount of experimental and theoretical PEM fuel cell work is being performed at *Los Alamos National Laboratories (LANL)*. Their modeling is of special interest because, in most cases, it is being rigorously coupled with experimental work. One of the groups led by Springer has contributed significantly to the understanding of the processes occurring in complete fuel cell assemblies. Their first one-dimensional, isothermal model which accounted for a partially dehumidified membrane was published in 1991 [6]. The anode catalyst layer is neglected and the cathode catalyst layer is assumed to be a thin reactive plane. The presence of liquid water in the electrodes is ignored. The result of this model predicts a net water per proton flux of 0.2 for typical operating conditions which compares well to their experimental measurements. They also show that significant advantages concerning cell performance result from using thinner membranes. In this study, the water content in the membrane had been measured experimentally as a function of relative humidity outside the membrane, and a correlation between the membrane conductivity and the humidification level of the membrane had been established. Since this is the only such model, it is still widely used by different authors when a partly humidified membrane is to be taken into account.

A more ambitious model examining water and thermal management in PEM fuel cells was developed by Fuller and Newman [7]. This quasi-two-dimensional model is obtained by solving a one-dimensional through-the-membrane problem and integrating the solutions at

various points in the down-the-channel direction. The model assumes that the oxidation of hydrogen and the evaporation of water are fast and can be neglected. The results of the work showed that the thermal considerations must be included in an analysis of water management.

A steady, two-dimensional heat and mass transfer model of a PEM fuel cell was presented in 1993 by Nguyen and White [8]. This model solves for the transport of liquid water through the membrane by electro-osmotic drag and diffusion and includes the phase-change of water, but the MEA is greatly simplified, assuming "ultra-thin" gas diffusion electrodes. The volume of the liquid phase is assumed to be negligible. This model was used to investigate the effect of different humidification schemes on the fuel cell performance. It was refined in 1998 by Yi and Nguyen [9] by including the convective water transport across the membrane, temperature distribution in the solid phase along the flow channel, and heat removal through natural convection and coflow and counterflow heat exchangers. The shortcoming of assuming ultrathin electrodes had not been addressed, so that the properties at the faces of the membrane are determined by the condition in channel. Again, various humidification schemes were evaluated. In 1999 Yi and Nguyen [10] published a two-dimensional model of the multi-component transport in the porous electrodes of an interdigitated gas distributor [11]. The first detailed two-phase model of a PEM fuel cell was published by He, Yi and Nguyen in 2000 [12]. It is two-dimensional in nature and employs the interdigitated flow field design proposed by Nguyen [11].

In the model proposed by Amphlett, Kim *et al.* they use an empirical equation to describe the performance curve of a PEM fuel cell over the complete operating range [13]. The inclusion of an exponential term with an adjustable parametric coefficient is found to

sophisticatedly model performance curves up to and including the mass transport limited region. The mechanistic insights of this equation are limited; however, the equation is of some use where a simple equation is needed to simulate cell performance. Such a application may be a complete fuel cell system.

In 1995, another PEM fuel cell model is published from a group at *Los Alamos* [14]. Weisbrod *et al.* developed an isothermal, steady-state, one-dimensional model of a complete cell incorporating the membrane water model of Springer *et al.* This model explores the possibility of the water flux in the electrode backing being a result of vapour flux only, or with liquid water present as well. If liquid water is present, they assume the gas stream is saturated. For the catalyst layer model, they assume that the catalyst particles are covered by a thin film of ionomer and that diffusion through this film can be neglected. The volume composition they use for the catalyst layer is dominated by void space. The results of the model indicate that moderate cell performance is predicted for catalyst loadings less then 0.1 mg/cm$^2$. The model also indicates a drop in performance when the cell temperature is raised to approximately 100°C with a gas stream pressure of 2 atm.

More recently, Wöhr *et al.* [15] have developed a one-dimensional model that is capable of simulating the performance of a fuel cell stack. In addition, it allows for the simulation of the transient effects after changes of electrical load or gas flow rate and humidification. For the membrane, the model previously described by Fuller and Newman [7] was used.

In 1998, the first model to use the methods of computational fluid dynamics (CFD) for PEM fuel cell modeling was published by Gurau *et al.* [16]. This group developed a two-dimensional, steady-state model of a whole fuel cell, *i.e.* both flow channels and the MEA

11

in between. The model considers the gas phase and the liquid phase in separate computational

domain, which means that the interaction between both phases is not considered.

Another research group to apply the methods of CFD for fuel cell modeling is located at

Pennsylvania State University. Their first publication [17] describes a two dimensional model

of a whole fuel cell similar to the one by Gurau *et al.*, with the exception the transient effects

can be included as well in order to model the response of fuel cell to a load change. This model

is used to investigate the effect of hydrogen dilution on the fuel cell performance. The transport

of liquid water through the membrane is included, but results are not shown. Since the model is

isothermal, the interaction between the liquid water and the water-vapour is not accounted for.

In a separate publication [18], the same group investigates the phase change at the cathode side

of a PEM fuel cell with a two-dimensional model. It is shown that for low inlet gas humidities,

the two-phase regime occurs only at high current densities. A multiphase mixture model is

applied here that solves for the saturation of liquid water, *i.e.* the degree of flooding.

The first fully three-dimensional model of a PEM fuel cell was published by a research

group from the University of South Carolina, where Dutta *et al.* used the commercial software

package *Fluent (Fluent, Inc.)* [19]. In this model, they accommodates an empirical membrane

model that can account for a partially dehydrated membrane. Two phase flow is also accounted

for, but in a simplified fashion that neglects the volume of the liquid water that is present inside

the gas-diffusion layer.

Overall it can be said that up to around 1998, most of the fuel cell models were

one-dimensional, focussing on the electrochemistry and mass transport inside the MEA. In

order to account for 2D and 3D effects, the methods of computational fluid dynamics have

recently been successfully applied to fuel cell modeling study.

## 1.5 Project Goal

The design for a fuel cell stack, thermal and water management subsystem, and the means of delivering fuel and oxidant are dependent upon the operating conditions of fuel cells. The optimum design point for a cell is determined by cell materials, transport properties, and reaction kinetics.

To decrease the costs of a PEM fuel cell system, optimization of cell design is required; ultimately, the power density needs to be increased. To this end, the goal of the project is to develop a comprehensive two-dimensional mathematical model for a complete PEM fuel cell in hope of sophisticatedly predicting the performance of a PEM fuel cell under various operating conditions. Particularly, a membrane sub-model that takes into account the three main transport mechanisms – diffusion of water, the pressure variation, and the electro-osmotic drag in the membrane, is formulated.

The outline of this project report is as follows: Chapter 2 introduces the chemical and thermodynamical theories of a fuel cell, fuel cell performance and efficiency definitions. From chapter 3 to chapter 6, the mathematical model of a complete PEM fuel cell is described on a component-by-component basis and the corresponding boundary conditions of this model are detailedly summarized in chapter 7. To sophisticatedly formulate the transport phenomena inside a PEM fuel cell, the properties and parameters are carefully selected from the available open literature and summarized in chapter 8. Finally, in chapter 9, conclusions are drawn and

an outline for future work is presented.

# Chapter 2 Fuel Cell Thermodynamics, Performance and Efficiencies

## 2.1 Introduction

The potential of a fuel cell at open circuit with no internal losses is know as the reversible cell potential, which is the maximum theoretical electric potential for a given reaction and can be determined by Nernst equation under the condition of thermodynamic equilibrium. Also the fuel cell performance characterized by overpotentical due to various mechanisms and efficiencies of a fuel cell are discussed in this chapter.

## 2.2 Fuel Cell Thermodynamics

### 2.2.1 Free-Energy Change of a Chemical Reaction

PEM fuel cells converse chemical energy into electrical energy directly by electrochemical reaction. For a general chemical reaction

$$\alpha A + \beta B \rightarrow \gamma C + \delta D \qquad (2.1)$$

the Gibb's free energy change is given in terms of chemical activities by:

15

$$\Delta \bar{g} = \Delta \bar{g}^0 + RT \ln \frac{a_C^\gamma a_D^\delta}{a_A^\alpha a_B^\beta} \qquad (2.2)$$

where $a_i$ is the chemical activity of the substance $i$ and the standard free energy change of the reaction, $\Delta \bar{g}^0$, is given by

$$\Delta \bar{g}^0 = -RT \ln \frac{a_{C,e}^\gamma a_{D,e}^\delta}{a_{A,e}^\alpha a_{B,e}^\beta} = -RT \ln K \qquad (2.3)$$

where the subscript $e$ 's in the activity terms indicate the values of the activities at equilibrium, and $K$ is the equilibrium constant for this reaction.

## 2.2.2 Free-Energy Change and Cell Potential: Nernst Equation

In this section the bridge between chemical activity and cell potential, Nernst equation, will be derived by considering a PEM fuel cell as an open system.
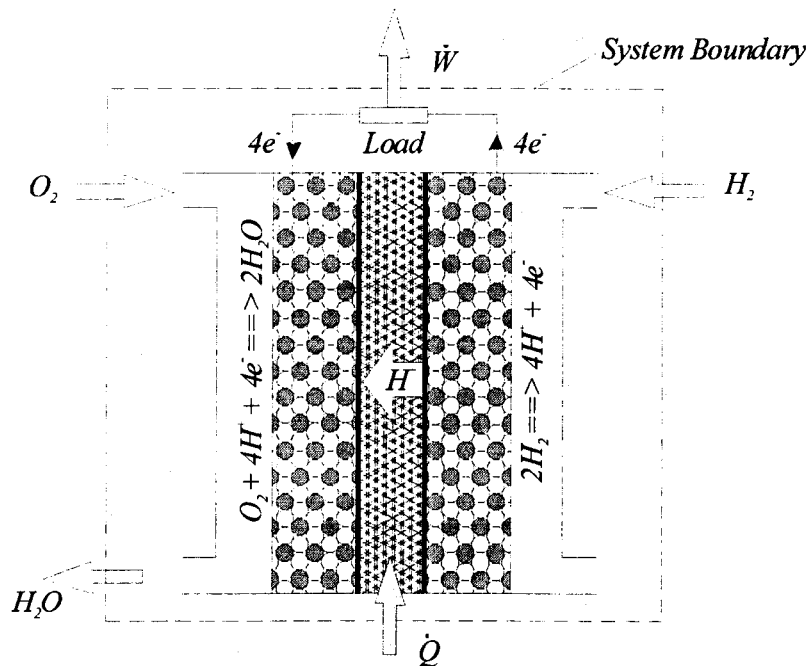


Figure 2 Open system boundary for thermodynamic consideration

16

Assuming an isothermal system and applying the first law of thermodynamics to the open system:

$$\dot{Q} - \Delta\dot{E} - \dot{W} = 0 \tag{2.4}$$

The internal energy change for an overall fuel cell reaction can be denoted as:

$$\Delta\dot{E} = \dot{n}_{H_2O}\overline{h}_{H_2O} - (\dot{n}_{H_2}\overline{h}_{H_2} + \dot{n}_{O_2}\overline{h}_{O_2}) \tag{2.5}$$

in equation (2.4) and (2.5), $\dot{n}_i$ s are the molar flow rates in [mol/s] and $\overline{h}$ is the molar enthalpy in [J/mol], $\dot{Q}$ and $\dot{W}$ represent the heat transferred to and work done by the system, respectively, in [W].

Substituting equation (2.5) into (2.4) and writing the expression on a *per mole of fuel* basis:

$$\overline{h}_{H_2} + \frac{\dot{n}_{O_2}}{\dot{n}_{H_2}}\overline{h}_{O_2} - \frac{\dot{n}_{H_2O}}{\dot{n}_{H_2}}\overline{h}_{H_2O} + \frac{\dot{Q}}{\dot{n}_{H_2}} - \frac{\dot{W}}{\dot{n}_{H_2}} = 0 \tag{2.6}$$

Recalling the overall fuel cell reaction:

$$2H_2 + O_2 \rightarrow 2H_2O \tag{2.7}$$

equation (2.6) can be written as:

$$\overline{h}_{H_2} + \frac{1}{2}\overline{h}_{O_2} - \overline{h}_{H_2O} + \frac{\dot{Q}}{\dot{n}_{H_2}} - \frac{\dot{W}}{\dot{n}_{H_2}} = 0 \tag{2.8}$$

or

$$\overline{h}_{in} - \overline{h}_{out} + \frac{\dot{Q}}{\dot{n}_{H_2}} - \frac{\dot{W}}{\dot{n}_{H_2}} = 0 \tag{2.9}$$

where $\bar{h}_{in}$ and $\bar{h}_{out}$ denote the incoming and outgoing enthalpy streams per mole of fuel, respectively.

Substituting the definition of Gibbs free energy, *i.e.*

$$\Delta \bar{g} = \Delta \bar{h} - T \Delta \bar{s} \qquad (2.10)$$

into equation (2.9) yields:

$$\frac{\dot{W}}{\dot{n}_{H_2}} = -(\Delta \bar{g} + T \Delta \bar{s}) + \frac{\dot{Q}}{\dot{n}_{H_2}} \qquad (2.11)$$

where $\Delta \bar{s}$ is the entropy change per mole of fuel and $T$ is the temperature in [K].

Rearranging (2.11) leads to

$$\bar{s}_{out} - \bar{s}_{in} - \frac{\dot{Q}/\dot{n}_{H_2}}{T} = -\frac{1}{T}(\Delta \bar{g} + \frac{\dot{W}}{\dot{n}_{H_2}}) \qquad (2.12)$$

note that the right hand side is always greater than zero.

If the process is carried out reversibly (*i.e.* equation (2.12) is equal to zero), we get the following expression for the heat production:

$$\frac{\dot{Q}}{\dot{n}_{H_2}} = T(\bar{s}_{out} - \bar{s}_{in}) \qquad (2.13)$$

By combining equation (2.9) and (2.13) we obtain an expression for the work of a reversible process, which is the maximum work obtainable from one mole of hydrogen:

$$\frac{\dot{W}}{\dot{n}_{H_2}} = \overline{h}_{in} - \overline{h}_{out} - T(\overline{s}_{in} - \overline{s}_{out}) \qquad (2.14)$$

or with the definition of the Gibb's free energy change, *i.e.* equation (2.10), the above equation can be written as:

$$\frac{\dot{W}}{\dot{n}_{H_2}} = g_{in} - g_{out} = -\Delta\overline{g} \qquad (2.15)$$

So we conclude that the free-energy change of a chemical reaction is a measure of the maximum net work obtainable from the reaction. For the overall reaction of a PEM fuel cell, the standard Gibb's free energy change is $\Delta\overline{g}^0 = -237.3 \times 10^3 \, J/mol$ when the product water is in the liquid phase [20].

Next, from the electrical view the reversible work in a fuel cell is the electrical work involved in transporting the charges around the circuit from the anode side towards the cathode side at their reversible potentials, $V_{rev,a}$ and $V_{rev,c}$, respectively. Hence, the maximum electrical work per mole of hydrogen provided by the overall reaction in a cell is:

$$\frac{\dot{W}_{rev}}{\dot{n}_{H_2}} = nF(V_{rev,c} - V_{rev,a}) \qquad (2.16)$$

where $F$ is the Faraday constant (96485 C mol$^{-1}$) and $n$ is the mole number of electrons per mole of hydrogen involving in the reaction.

Comparing equation (2.16) with (2.15) results in:

$$\Delta\overline{g} = -nF(V_{rev,c} - V_{rev,a}) \qquad (2.17)$$

*i.e.*

$$\Delta \bar{g} = -nFE_{rev}$$ (2.18)

where $E_{rev}$ is the electromotive force (EMF) of the cell.

Under the standard state, it follows that

$$\Delta \bar{g}^0 = -nFE^0{}_{rev}$$ (2.19)

where terms with superscript "0" represent "standard state".

Combining these equations with (2.2) yields:

$$E_{rev} = -\frac{\Delta \bar{g}^0}{nF} - \frac{RT}{nF} \ln \frac{a_C^\gamma a_D^\delta}{a_A^\alpha a_B^\beta}$$ (2.20)

which reduced to the common form of the so-called *Nernst Equation*:

$$E_{rev} = E_{rev}^0 - \frac{RT}{nF} \ln \frac{a_C^\gamma a_D^\delta}{a_A^\alpha a_B^\beta}$$ (2.21)

In the case of the hydrogen-oxygen fuel cell the *Nernst equation* results in:

$$E_{rev} = E_{rev}^0 - \frac{RT}{2F} \ln \frac{a_{H_2O}}{a_{H_2} a_{O_2}^{1/2}}$$ (2.22)

which allows the computation of theoretical cell potentials for a fuel cell.

When considering the effect of temperature on the free energy change, the above equation becomes:

$$E_{rev,T} = E_{rev}^0 - \frac{\Delta \bar{s}^0}{2F}(T - T^0) - \frac{RT}{2F} \ln \frac{a_{H_2O}}{a_{H_2} a_{O_2}^{1/2}}$$ (2.23)

where the activities can be replaced by the partial pressures for ideal gases, *i.e.*

$$a_i = p_i / p \qquad (2.24)$$

with $p_i$, $p$, the partial pressure of gaseous species $i$ and the pressure of the gaseous mixture, respectively.

## 2.3 Fuel Cell Performance

Fuel cell potential predicted by Nernst equation is under the condition of equilibrium. The actual cell potential under operating conditions is always smaller than it. Figure 3 shows a typical polarization curve of a PEM Fuel Cell.
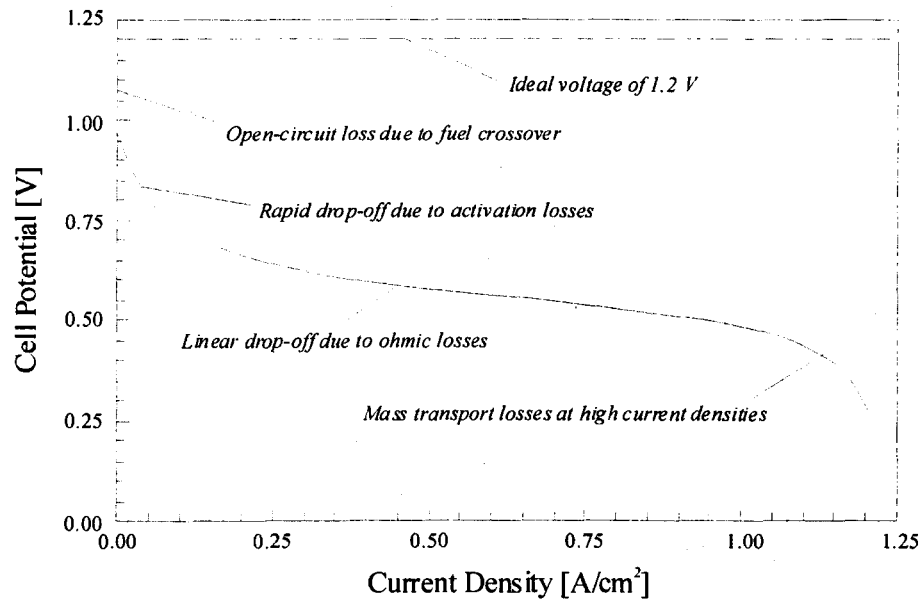


Figure 3 Typical polarization curve of a PEM fuel cell and predominant loss mechanisms in various current density regions

The potential losses in a PEM fuel cell are usually due to the following reasons:

- **Fuel crossover or internal currents** occurs due to the diffusion of hydrogen across the membrane and recombining with the oxygen on the cathode side;

- **Activation losses** are caused by the slowness of the reactions taking place on the surface of the electrodes. In a PEM fuel cell this loss occurs mainly on the cathode side since the exchange current density of the anodic reaction is several orders of magnitude higher than that of the cathodic reaction. In most cases, the applied activation overpotential is described by Tafel equation [21];

- **Ohmic losses** result from the resistance of the electrolyte (membrane for PEM fuel cell) and sometimes the electrical resistance of the electrodes;

- **Mass transport or concentration losses** result from the change in concentration of the reactants at the surface of the electrodes as the reactants are being consumed. It becomes significant when the cell is working at a relatively higher current density.

## 2.4 Fuel Cell Efficiencies

**The Maximum Intrinsic Efficiency**

From the thermodynamic view, the intrinsic maximum efficiency is given by:

$$\varepsilon_i = \frac{\Delta \bar{g}}{\Delta \bar{h}} = 1 - \frac{T \Delta \bar{s}}{\Delta \bar{h}} = -\frac{nF}{\Delta \bar{h}} E_{rev} \tag{2.25}$$

which can be used to compare with other energy conversion devices.

**Voltage Efficiency**

Under the working condition the terminal cell potential of a fuel cell decreases with increasing current density drawn from the cell due to the following reasons:

- The slowness of one or more of the intermediate steps of the reactions occurring at either or both of the electrodes;

- The slowness of mass transport processes;

- Ohmic losses through the electrolyte.

So the terminal cell potential can be given by:

$$E = E_{rev} - \eta_{act,a} - \eta_{act,c} - \eta_{conc,a} - \eta_{conc,c} - \eta_{ohm} \qquad (2.26)$$

where the $\eta's$ with the appropriate subscripts represent the magnitudes of the losses of the first two types at the anode $a$ and the cathode $c$ and the third type generally in the electrolyte.

Then the voltage efficiency $\varepsilon_e$ is defined as:

$$\varepsilon_e = \frac{E}{E_{rev}} \qquad (2.27)$$

**The Faradaic Efficiency**

Due to the fact that either there is an incomplete conversion of the reactants at each electrode to their corresponding products or sometimes cross-over effect, there will be a portion of losses, which is taken into account by the faradaic efficiency, and it is defined as:

$$\varepsilon_f = \frac{I}{I_{theo}}$$ (2.28)

where $I$ is the observed current from the cell and $I_{theo}$ is the theoretically expected current

on the basis of the amount of reactants consumed, assuming that the overall reaction in the fuel

cell proceeds to completion.

**Fuel Utilization Efficiency**

In practice, to keep a finite concentration gradient in a fuel cell, which is needed to allow

the reactants to diffuse towards the catalyst layer, extra amount of fuel has to be input. A fuel

utilization coefficient can be defined as:

$$\vartheta_f = \frac{\text{mass of fuel reacted in cell}}{\text{mass of fuel input into cell}}$$ (2.29)

note that this is the inverse of the stoichiometric flow ratio.

**Overall Efficiency**

The overall efficiency $\varepsilon$ in a fuel cell is the product of the efficiencies worked out in the

preceding subsections:

$$\varepsilon = \vartheta_f \varepsilon_i \varepsilon_e \varepsilon_f$$ (2.30)

# Chapter 3 Gas Flow Channel Model

## 3.1 Introduction

The gas flow channels in a PEM fuel cell are curved into bipolar plates, and serve the purposes of feeding oxygen to the cathode and fuel gas to the anode. The commonly used material of bipolar plates is graphite, which is also a good electrical conductor for current collection. In a PEM fuel cell, bipolar plates make up the majority of the volume because anode, electrolyte and cathode are made in one very thin piece. Meanwhile, significant amount of cost has to be considered because of the complexity and difficulty of bipolar plate manufacture.

To make the gas transport more efficient, the design of the gas flow channel is usually much more complicated than the simple straight channels. However in this project such a simple straight channel model is still used since it is capable of providing reasonable prediction for the processes occurring within a PEM fuel cell in spite of its simplicity.

25

## 3.2 Assumptions

The gas flow channel model presented in this chapter is based on the following assumptions:

1. the transport processes are steady-state and two-dimensional;

2. two ternary gaseous systems, $O_2$, $N_2$ and $H_2O_g$ on the cathode side and $H_2$, $CO_2$ and $H_2O_g$ on the anode side, will be considered in this model;

3. all gases are assumed to be ideal gases;

4. the flow in the channels is considered laminar;

5. all gases are assumed to be fully compressible and saturated with water vapour;

6. the effect of gravity is neglected;

## 3.3 Mathematical Formulation

In fuel cell channels, only the gas-phases are considered. The various transport processes occurring in the flow channel are mathematically described by applying the following generic steady-state *Navier-Stokes* equations in their compressible form:

the continuity equation:

$$\nabla \cdot (\rho_g \vec{U}_g) = 0 \qquad (3.1)$$

the momentum equations:

in x direction:

$$\rho_g(\vec{U}_g \cdot \nabla)u_g = -\frac{\partial p}{\partial x} - \left(\frac{\partial \sigma_{xx}}{\partial x} + \frac{\partial \sigma_{yx}}{\partial y}\right) \tag{3.2}$$

in y direction:

$$\rho_g(\vec{U}_g \cdot \nabla)v_g = -\frac{\partial p}{\partial x} - \left(\frac{\partial \sigma_{xy}}{\partial x} + \frac{\partial \sigma_{yy}}{\partial y}\right) \tag{3.3}$$

the energy equation:

$$-\nabla \cdot (\lambda_g \nabla T_g) + \nabla \cdot (\rho_g \vec{U}_g H) = 0 \tag{3.4}$$

In the continuity equations (3.1), $\rho_g$ and $\vec{U}_l = (u_g, v_g)^t$ are the density and velocity of the gaseous mixture, respectively. The subscript "g" denotes the gas-phase here.

In the two momentum equations, *i.e.* (3.2) and (3.3), $p_g$ is the pressure of the fluid, and $\sigma_{xx}$, $\sigma_{yy}$ and $\sigma_{xy}$ are components of stress tensor expressed as:

$$\sigma_{xx} = -2\mu\frac{\partial u_g}{\partial x} + (\frac{2}{3}\mu - \xi)\left(\frac{\partial u_g}{\partial x} + \frac{\partial v_g}{\partial y}\right) \tag{3.5}$$

$$\sigma_{yy} = -2\mu\frac{\partial v_g}{\partial y} + (\frac{2}{3}\mu - \xi)\left(\frac{\partial u_g}{\partial x} + \frac{\partial v_g}{\partial y}\right) \tag{3.6}$$

$$\sigma_{xy} = \sigma_{yx} = -\mu\left(\frac{\partial u_g}{\partial x} + \frac{\partial v_g}{\partial y}\right) \tag{3.7}$$

with $\mu$, dynamic viscosity, and $\xi$, dilatational viscosity.

In the energy conservation equation, $\lambda_g$ is the thermal conductivity of gaseous mixture and $H$ is the total enthalpy calculated out of the static (thermodynamics) enthalpy $h$ via:

$$H = h + \frac{1}{2}\left|\vec{U}_g\right|^2 \tag{3.8}$$

There are seven unknowns involving in equation (3.1) – (3.4) and (3.8): $\rho_g$, $u_g$, $v_g$, $p_g$,

$T_g$, $H$ and $h$ , which are used to describe the behaviour of bulk flow instead of those for a certain individual species in the mixture.

To make the system complete, the other two algebraic equations from thermodynamics should be added. One is the constitutive equation, relating static enthalpy to temperature and pressure. For our assumed thermally perfect fluid, $h$ is a function of temperature only, that is:

$$\Delta h = c_p \Delta T_g \tag{3.9}$$

where $c_p$ is specific heat capacity at constant pressure and is approximately viewed as a constant here. The other auxiliary equation is the state equation relating density to temperature and pressure. For each ideal gaseous species $i$ in the ternary gaseous system, it obeys:

$$\rho_i = \frac{p_g M_i}{R T_g} \tag{3.10}$$

where $M_i$ is the molecular weight of species $i$, and $R$ is the universal gas constant (8.3143 J/mol-K).

The relationship between the average density $\rho_g$ and the densities of components in the mixture, $\rho_i$, is:

$$\frac{1}{\rho_g} = \sum_{i=1}^{3} \frac{\omega_i}{\rho_i} \tag{3.11}$$

where $\omega_i$ is the mass fraction of the species $i$ in the mixture.

In addition, each species obeys the following generic advective-diffusive mass transfer equation:

$$-\nabla \cdot (\Gamma_{gi} \nabla \omega_{gi}) + \nabla \cdot (\vec{U}_g \rho_g \omega_{gi}) = 0 \tag{3.12}$$

where the first term in the left-hand side denotes the mass transfer due to diffusion and the second term represents that due to convection. In equation (3.12), $\Gamma_{gi}$ is the molecular diffusion coefficient for species $i$.

In a binary mixture of two species, say $A$ and $B$, we have $\Gamma_{gA} = \Gamma_{gB} = \rho D_{AB}$, where $D_{AB}$ is the binary diffusivity of species $A$ in species $B$. However for a ternary mixture system considered in our model the diffusion becomes more complex, because the diffusive flux now is a function of the concentration gradient of two species instead of only one kind. The way chosen here to deal with the problem is to approximately view the ternary system as the mixture made from three existing binary pairs - $O_2$ and $N_2$, $N_2$ and $H_2O_g$, $H_2O_g$ and $O_2$ in the cathode-side channel, and the similar treatment can be applied to the anode-side channel. Thus, each binary pair can be considered as a binary mixture so that we can treat the ternary mixture by simply using binary-mixture-related approach.

So far, the mathematical model describing bulk physical quantities of our interest, *i.e.* $\vec{U}_g$, $\rho_g, p_g$, $T$ and $\omega_{gi}$, have been presented. Considering that saturation pressure varies with temperature, thus the variation of vapor content in the mixture, we should perform some updates to sophisticatedly account for the concentration variation of each species.

In practice, the relationship between saturation pressure and temperature can be obtained using the empirical formula [6]:

$$p_g^{sat} = 10^{(-2.1794+0.02953T-9.1837\times10^{-5}T^2+1.4454\times10^{-7}T^3)} \tag{3.13}$$

with the temperature $T$ in [°C].

This new saturation pressure from temperature correction equation (3.13) will be used to

calculate the molar fraction of water vapour in the gas flow channel:

$$X_{H_2O_g} = \alpha \frac{p_g^{sat}}{p_g} \tag{3.14}$$

where $\alpha$ is the relative humidity, which is unity if the gaseous mixture is fully humidified.

Then the mass fraction of vapour can be obtained using:

$$\omega_{H_2O_g} = \frac{X_{H_2O_g} M_{H_2O_g}}{\sum_{j=1}^{3} X_{gi} M_i} \tag{3.15}$$

The newly updated vapor mass fraction will be back-substituted into (3.12) to update mass fraction $\omega_i$ for other species. Particularly, accurate concentration distributions of $H_2$ and $O_2$, which are of importance in optimization and design of PEM fuel cell, can be obtained.

Finally, to investigate diffusion details of each species of the ternary system, the *Stefan-Maxwell* equation is included [22]:

$$\nabla X_{gi} = -\sum_{j=1(j \neq i)}^{3} \frac{X_{gi} X_{gj}}{D_{ij}} (\vec{U}_i - \vec{U}_j) \tag{3.16}$$

where $\vec{U}_i$ is the diffusion velocity of species $i$ defined as:

$$\vec{U}_i = \vec{u}_i - \vec{U}_g \tag{3.17}$$

with $\vec{u}_i$, the absolute velocity of species $i$. $D_{ij}$ is the binary diffusivity for each above-mentioned binary pair; $X_{gi}$ is the molar fraction of $i^{th}$ species in the gas mixture and it can be obtained from mass fraction using following expression:

$$X_{gi} = \frac{\omega_{gi}/M_i}{\sum_{j=1}^{3} \omega_{gj}/M_j} \tag{3.18}$$

# Chapter 4 Electrode Model

## 4.1 Introduction

The gas diffusion electrodes (GDE) consist of carbon cloth or carbon fibre paper and they serve to transport the reactant gases towards the catalyst layer through the open wet-proofed pores. Meanwhile, they provide interfaces where ionization takes place and the solid matrix through which electrons are transferred to outer circuit to provide electrical power. In addition, for contemporary PEM fuel cell, the electrode structure often incorporates a layer of platinum black or platinum supported catalyst. It is the place where electrochemical reaction occurs. In this project, this region is modeled as a separate layer and will be described in the next chapter.

The aim of the electrode model is to quantify the effects of specified operating conditions on heat and mass transfer of the gaseous species in the porous electrode, which is of importance in determining the resulting cell performance. Particularly, in this region of the PEM fuel cell the effects of flooding may limit transport of gaseous reactants towards the reaction sites, thereby starving the cell. Thus, understanding the transport of water as vapour and liquid is very important to PEM fuel cell design and optimization. This can be achieved by modeling the effect of energy variation within the computation domain.

## 4.2 Assumptions

Except those we have made in the previous chapter, the following assumptions for the electrode model are adopted to make the analysis tractable:

1. the water in the pores of the gas diffusion electrodes is considered separate from the gases, *i.e.*, the gas and liquid water are at different pressure;

2. no phase change is taken into account for the reason of simplicity;

3. the dissipation effect of viscosity are neglected because the primary means of gas transport is diffusion in porous electrodes;

4. the convective heat transfer between solid matrix of the gas-diffusion-electrode and gas mixture is negligible;

## 4.3 Mathematical Formulation

The equations that govern the transport phenomena in the diffusion electrode layers are similar to those in the gas flow channel, except that the gas-phase porosity $\gamma_g$ of the electrode material should be additionally taken into account. The continuity equation for gas-phase is given in compressible form:

$$\nabla \cdot (\rho_g \gamma_g \vec{U}_g) = 0 \tag{4.1}$$

and the momentum equations reduce to Darcy's law:

$$\gamma_g \vec{U}_g = -\frac{k_{g,p}}{\mu_g} \nabla p_g \tag{4.2}$$

where $k_{g,p}$ is the gas-phase hydraulic permeability and $\mu_g$ denotes the viscosity of the gaseous mixture in porous electrodes.

Since the gas and liquid have their own pressure (assumption 1) in porous electrodes, the mass conservation equation for the liquid water takes the following incompressible form, *i.e.*:

$$\nabla \cdot (\gamma_l \vec{U}_l) = 0 \tag{4.3}$$

meanwhile, the Darcy's law is applied to liquid water as well:

$$\gamma_l \vec{U}_l = -\frac{k_{l,p}}{\mu_l} \nabla p_l \tag{4.4}$$

where $k_{l,p}$ is the liquid water hydraulic permeability and $\mu_l$ denotes the viscosity of liquid water in porous electrodes. Note that the subscript " $l$ " represents "liquid water" here.

The effect due to porosity of electrodes has to be taken into account in the energy equation:

$$-\nabla \cdot (\lambda_g^{eff} \nabla T_g) + \nabla \cdot (\rho_g \gamma_g \vec{U}_g H) = 0 \tag{4.5}$$

where, $\lambda_g^{eff}$ is the effective thermal conductivity, which has considered the effect of porosity and the conductivity of electrode material. The convective heat transfer between solid matrix of the gas-diffusion-electrode and gas mixture is not considered due to assumption 4.

The corresponding generic advective-diffusive mass transfer equation for different gaseous species can be given as:

$$-\nabla \cdot (\Gamma_{gi} \gamma_g \nabla \omega_{gi}) + \nabla \cdot (\vec{U}_g \rho_g \gamma_g \omega_{gi}) = 0 \tag{4.6}$$

Similar to the gas flow channel model, the diffusion details of each species in electrode model can be obtained by solving porosity-corrected *Stefan-Maxwell* equations.

33

# Chapter 5 Catalyst Layer Model

## 5.1 Introduction

The catalyst layer is the place where fuel and oxidant react electrochemically to produce electrical work. The composition, morphology, and thickness of catalyst layer are critical in determining the performance and the resulting cost of a PEM cell. Extensive research in catalyst layer morphology is being conducted in hopes of reducing the amount of precious metal catalyst required and decreasing polarizations in this layer.

Because of the small physical dimensions of membrane thickness and the simplification needs due to the complexities of physical and chemical processes, the catalyst layers, in this project, are assumed to be interfaces with certain source and/or sink terms to meet the heat and mass balance requirements of other modeling equations.

## 5.2 Assumptions

Except the sink/source terms assumption, to simplify the problem, we also have the following ones:

34

1. all gaseous water completely condense at the catalyst layer interfaces: that means all water in the membrane is in the liquid phase;

2. the reaction kinetics is taken to be first order and thus can be described by the *Bulter-Volmer* equation [23];

3. the catalyst distribution is uniform throughout the entire layer: this is the requirement of homogenous source/sink term assumption;

## 5.3 Mathematical Formulation

Based on the overall chemical reaction relations given by (2.7), the local sink term for hydrogen can be expressed by a function of the local current density $\vec{i}$ :

$$S_{H_2} = -\frac{\nabla \cdot \vec{i}}{2F} M_{H_2} \tag{5.1}$$

where $M_{H_2}$ is the molecular weight of hydrogen and $F$ is the Faraday constant. The negative sign here represents "sink" or "consume".

Similar to the hydrogen depletion at the anode side, the local oxygen depletion at the cathode side is described as:

$$S_{O_2} = -\frac{\nabla \cdot \vec{i}}{4F} M_{O_2} \tag{5.2}$$

From the equation above, it can be seen how important it is to obtain a sophisticated description of the local current density $i$. This can be given by *Bulter-Volmer* equation based on

the assumption 2 [23]:

$$i = i_0 \left[ \exp\left( \frac{\beta_a F}{RT} \eta_{act} \right) - \exp\left( -\frac{\beta_c F}{RT} \eta_{act} \right) \right] \tag{5.3}$$

where $i_0$ is the apparent exchange current density; $\beta_a$ and $\beta_c$ are the anodic and cathodic apparent transfer coefficients, respectively; $F$ is Faraday constant and $\eta_{act}$ is the activation overpotential.

Typically, the reaction at the cathode is slow and therefore requires a higher polarization than the anode does to satisfy a given current density. Since the activation overpotential at the cathode catalyst layer is highly negative, one of the terms on the right-hand side of equation (5.3) can be neglected:

$$i = -i_0 \left[ \exp\left( -\frac{\beta_c F}{RT} \eta_{act} \right) \right] \tag{5.4}$$

The apparent exchange current density $i_0$ is a function of the temperature and the reactant concentrations as well as the catalyst loading [8]. The relation between the exchange current density and the dissolved gas concentrations at the cathode catalyst layer is given by [24]:

$$i_0 = i_0^{ref} \left( \frac{c_{O_2}}{c_{O_2}^{ref}} \right)^{\gamma_{O_2}} \left( \frac{c_{H^+}}{c_{H^+}^{ref}} \right)^{\gamma_{H^+}} \tag{5.5}$$

The concentration of protons throughout the catalyst layer is fixed by the concentration of negative charge sites in the membrane, and it can be assumed constant. Therefore, the second term on the right-hand side is equal to unity yielding:

$$i_0 = i_0^{ref} \left( \frac{c_{O_2}}{c_{O_2}^{ref}} \right)^{\gamma_{O_2}} \tag{5.6}$$

where $i_0^{ref}$ is the reference exchange current density and it is one of the input parameters of this model.

From the equation above, it is important to note that for constant activation overpotential, the local current density is a function of the local reactant concentration. For example on the cathode side it holds that:

$$i = i_{ave} \left( \frac{x_{O_2}}{x_{O_2,ave}} \right)^{\gamma_{O_2}} \tag{5.7}$$

where $i_{ave}$ is the average current density and $x_{O_2,ave}$ is the average oxygen concentration at the catalyst layer. Hence, the local current distribution for a desired current density can be determined by knowledge of the local oxygen concentration distribution and average oxygen concentration at the catalyst layer.

Then, to complete the mathematical description of energy transport in the previous chapters, the energy source term due to chemical reaction and overall ohmic effect has to be taken into account:

$$\dot{q}_r = \frac{\Delta H_r}{4F} i + V_{cell} i \tag{5.8}$$

where $\Delta H_r$ is the enthalpy change of reaction and $V_{cell}$ is the cell voltage. The second term on the right-hand side takes account of heat generated due to ohmic effect.

We have assumed that all the gaseous water condense at catalyst layers, so the liquid water source terms must be given accordingly. Meanwhile, there is liquid water generated on cathode

side due to the chemical reaction, leading to an extra water source term at cathode-side catalyst layer:

$$S_{H_2O,c} = \nabla \cdot (\frac{\vec{i}}{2F} + \vec{N}_{H_2O_g}) M_{H_2O} \qquad (5.9)$$

and at anode-side catalyst layer:

$$S_{H_2O,a} = (\nabla \cdot \vec{N}_{H_2O_g}) M_{H_2O} \qquad (5.10)$$

where $\vec{N}_{H_2O_g}$ is the molar flux of water vapor from electrodes.

# Chapter 6 Membrane Model

## 6.1 Introduction

The categorization of fuel cells is usually based upon the type of electrolyte. For a PEM fuel cell, a perfluorosulfonate polymer membrane is usually chosen to act as a hydrogen ion conductor. Membranes from different manufacturer have differing characteristics, but a common point is that they all seem to exhibit minimum resistance to proton transport when saturated with water. Thus, it is particularly important to maintain appropriate water content in the electrolyte membrane.

Water transport in membrane is driven by three mechanisms: diffusion due to the concentration gradient of water, pressure gradient due to the difference between anode and cathode inlet pressure and electro-osmotic effect due to the drag force caused by proton migration in membrane. At low current densities the electro-osmotic drag is not significant, and therefore the trend of water transport is from Cathode to anode side. While, with the current densities increasing, the electro-osmotic drag becomes dominant and water begin to transport in the reverse direction. This will lead to membrane dehydration at anode side. The situation will be further deteriorated when heat generated by the exothermic electrochemical reaction at

the cathode is considered. In practice, maintaining the membrane near full saturation is usually achieved by carefully balancing the supply and removal of water vapor to ensure that neither flooding of the electrodes nor drying out of the membrane takes place.

In the project, our focus is placed on the study of partial hydration in the membrane by developing a membrane model, which partially based on empirical relationship proposed by Springer *et al.* [6, 25] to account explicitly for water diffusion, pressure distribution, and electro-osmotic drag; meanwhile, thermal effects are introduced implicitly via the variation of membrane transport parameters as functions of temperature.

## 6.2 Assumptions

The following assumptions are made for the membrane model:

1. no phase change is considered in membrane;

2. hydrogen and oxygen species are not present in the layer: that means, only two mobile species, liquid water and proton, are considered in the membrane;

3. the pressure variation is linear across the membrane: it is unknown what the actual pressure distribution in the membrane is , however, this is felt to be a suitable first assumption;

## 6.3 Mathematical Formulation

The membrane model is mathematically described by considering the mass conservation for the two mobile species: liquid water and proton.

## 6.3.1 Water Transport in Membrane

For liquid water transport in membrane, the following mass conservation principle, under the condition of steady-state, should be obeyed:

$$\nabla \cdot \vec{N}_w = 0 \tag{6.1}$$

where $\vec{N}_w$ is the molar flux of water across the membrane.

The net flux of water across the membrane is assumed to be the sum of osmotic-drag, diffusion, and convection due to a pressure gradient:

$$\vec{N}_w = -D_w \nabla c_w - c_w \varepsilon_w^m \frac{k_h}{\mu_l} \nabla p_l + \frac{n_d \vec{i}}{F} \tag{6.2}$$

where, $c_w$ is the molar concentration of water, which is the variable of our interest; $D_w$ is the diffusion coefficient; the parameters $k_h$ and $\mu_l$ are the hydraulic permeability of the membrane and water viscosity respectively; $\varepsilon_w^m$ is the water volume fraction in the membrane; $n_d$ is the electro-osmotic drag coefficient, which is defined as the molar number of water transported by a mole of protons under the condition of no concentration and pressure gradient; $\vec{i}$ is the current density. Note that the subscript "$w$" represents "liquid water".

Current conservation law gives:

$$\nabla \cdot \vec{i} = 0 \tag{6.3}$$

and according to the linear pressure distribution assumption 3, we have:

$$\nabla^2 p = 0 \tag{6.4}$$

Using relations (6.3) and (6.4), the divergence of net water flux (6.2) is reduced to:

$$\nabla \cdot \vec{N}_w = -D_w \nabla^2 c_w - \varepsilon_w^m \frac{k_h}{\mu_l} (\nabla c_w \cdot \nabla p_l) + \frac{\nabla n_d \cdot \vec{i}}{F} \tag{6.5}$$

where the variation of water volume fraction $\varepsilon_w^m$ and water diffusion coefficient $D_w$ are relatively small and can be considered as a constant during the derivation.

Thus, from (6.1), we get:

$$-D_w \nabla^2 c_w - \varepsilon_w^m \frac{k_h}{\mu_l} (\nabla c_w \cdot \nabla p_l) + \frac{\nabla n_d \cdot \vec{i}}{F} = 0 \tag{6.6}$$

Next, based on the work of Springer *et al.* [6] who propose a functional relationship between electro-osmotic drag coefficient and the membrane water content, the third term in the above equation will be further developed.

Their experiment examining Nafion 117 shows a simple linear relationship between electro-osmotic drag coefficient and water content $\lambda$, which is defined as the number of moles of water per equivalent sulfonic acid group, $SO_3^-$, in the membrane:

$$n_d = \frac{2.5}{22} \lambda \tag{6.7}$$

which indicates that Nafion 117 exhibits $n_d = 2.5$ for $\lambda = 22$.

An empirical formula relating $c_w$ to $\lambda$ is also presented by Springer *et al.*:

$$c_w = \frac{e\lambda}{f\lambda + 1} \tag{6.8}$$

where, $f$ is an experimentally determined swelling constant coefficient for the membrane

and $e$ is a constant property for Nafion 117, which is given by:

$$e = \frac{\rho_m^{dry}}{E_m}$$ (6.9)

with $\rho_m^{dry}$, dry membrane density, and $E_m$, equivalent membrane weight.

Rearranging equation (6.8) leads to:

$$\lambda = \frac{c_w}{e - fc_w}$$ (6.10)

Substituting (6.10) back into (6.7), we can get an empirical expression for the electro-osmotic drag coefficient $n_d$ as:

$$n_d = \frac{2.5}{22} \frac{c_w}{e - fc_w}$$ (6.11)

The gradient of $n_d$ can be obtained as:

$$\begin{aligned} \nabla n_d &= \nabla(\frac{2.5}{22} \frac{c_w}{e - fc_w}) \\ &= \frac{5}{44} \frac{(e - fc_w)\nabla c_w + c_w f \nabla c_w}{(e - fc_w)^2} \\ &= \frac{5}{44} \frac{e\nabla c_w}{(e - fc_w)^2} \end{aligned}$$ (6.12)

Finally, the equation (6.6) can be rewritten in term of water concentration as:

$$-D_w \nabla^2 c_w - \varepsilon_w^m \frac{k_h}{\mu_l}(\nabla c_w \cdot \nabla p_l) + \frac{5}{44} \frac{e(\nabla c_w \cdot \bar{i})}{F(e - fc_w)^2} = 0$$ (6.13)

which is a complete mathematical description of water concentration distribution in membrane.

Given the pressure profile $p_l$ and current density $\vec{i}$, the above equation can be viewed as an nonlinear partial differential equation of $c_w$. By applying appropriate boundary condition, the distribution of water concentration in membrane can be obtained. This will be a good starting point for the potential distribution study in the membrane, because, as has been mentioned, the proton transport is directly related to the water transport in the membrane.

### 6.3.2 Proton Transport in Membrane

Similar to water transport, proton transport in membrane also obeys the following mass conservation principle, under the condition of steady-state:

$$\nabla \cdot \vec{N}_p = 0 \qquad (6.14)$$

where $\vec{N}_p$ is the molar flux of proton across the membrane.

The proton transport in membrane can be mathematically described by *Nernst-Planck equation*, which indicates that the net flux of proton across the membrane is assumed to be the sum of migration, diffusion, and convection of the dissolved protons [4, 26 and 27]:

$$\vec{N}_p = -Z_p \frac{F}{RT} D_p c_p \nabla \phi - D_p \nabla c_p + c_p \vec{U}_l \qquad (6.15)$$

with $Z_p$, the charge number of proton, $D_p$, the proton diffusion coefficient, $c_p$, the molar concentration of protons, $\phi$, the electrical potential and $\vec{U}_l$, the convective velocity of the liquid water. Note the subscript " $p$ " represents "proton".

The mathematical description of liquid water velocity in membrane pores can be estimated by *schlögl equation* [26, 27]:

$$\vec{U}_l = \varepsilon_w^m (\frac{k_\phi}{\mu_l} Z_f c_f F \nabla \phi - \frac{k_p}{\mu_l} \nabla p_l) \qquad (6.16)$$

where $k_\phi$ and $k_p$ denote the electric and hydraulic permeabilities, respectively; $Z_f$ is the charge number of the fixed-charges; $c_f$ is the fixed-charge concentration in the membrane; F is Faraday constant and $\mu_l$ is the liquid water viscosity.

This equation considers two different water transport mechanisms: the electro-osmotic drag, whereby protons migrating through the membrane drag water molecules with them, and pressure driven flux, which is usually directed from the cathode side to the anode side. Strictly speaking, a diffusive term should be accounted for as well, however, comparing with the migration and pressure gradient effects, this term is neglected to simplify the model formulation. In addition, one should note that under the steady state, we have:

$$\nabla \cdot \vec{U}_l = 0 \qquad (6.17)$$

Since the flux of charged species constitutes an electric current, the current density in an electrolytic solution (*i.e.* membrane in our case) can be given as:

$$\vec{i} = F \sum Z_i \vec{N}_i \qquad (6.18)$$

where $\vec{N}_i$ and $Z_i$ are the molar flux and the charge number of charged mobile ion of species $i$ in the membrane, respectively.

For PEM fuel cell, the only charged mobile ion in the membrane is proton ($Z_p = 1$), so we have:

$$\vec{i} = F \vec{N}_p \qquad (6.19)$$

and the membrane conductivity generally defined as:

$$\kappa = \frac{F^2}{RT} \sum Z_i^2 D_i c_i \qquad (6.20)$$

reduces to:

$$\kappa = \frac{F^2}{RT} D_p c_p \qquad (6.21)$$

For a macroscopic portion of a cell, the fact that there should be no net charge gives the electro-neutral principle:

$$\sum z_i c_i = 0 \qquad (6.22)$$

and for PEM fuel cell (proton and fixed charge are the only two charged species) it can be written as:

$$Z_f c_f + c_p = 0 \qquad (6.23)$$

Using the above relationships, the *Nernst-Planck equation* (6.15) and *schlögl equation* (6.16) can be rewritten as:

$$\vec{N}_p = -\frac{F}{RT} D_p c_p \nabla \phi - D_p \nabla c_p + c_p \vec{U}_l \qquad (6.24)$$

and

$$\vec{U}_l = -\varepsilon_w^m (\frac{k_\phi}{\mu_l} c_p F \nabla \phi + \frac{k_p}{\mu_l} \nabla p_l) \qquad (6.25)$$

Combination of equation (6.17), (6.19), (6.21), (6.24), (6.25) along with the proton transport conservation condition (6.14) gives:

$$-\nabla^2\phi = -\frac{1}{\kappa}(\nabla(\ln c_p)\cdot\vec{i}) + \frac{RT}{F}\nabla\cdot(\nabla(\ln c_p)) \tag{6.26}$$

which relates the potential distribution in the membrane to the proton concentration variation.

The proton concentration $c_p$ varies with the variation of hydration in the membrane and the functional relation between them is needed to construct the electrical potential equation in term of water concentration. Similar to the equation (6.8), for Nafion 117 the proton concentration can be described as:

$$c_p = \frac{e}{f\lambda + 1} \tag{6.27}$$

where $e$ and $f$ have the same physical meanings with those mentioned before.

Comparing equation (6.27) and (6.8), we can get the relation between the two concentration variables as follow:

$$c_p = e - fc_w \tag{6.28}$$

Substituting (6.28) into (6.26), we get the electrical potential expression in term of water concentration $c_w$ :

$$-\nabla^2\phi = \frac{1}{\kappa}\frac{f}{e-fc_w}(\nabla c_w\cdot\vec{i}) - \frac{RT}{F}\frac{f}{e-fc_w}\nabla^2 c_w - \frac{RT}{F}\left(\frac{f}{e-fc_w}\right)^2 (\nabla c_w\cdot\nabla c_w) \tag{6.29}$$

Then, by substituting equation (6.13) into equation (6.29), we can get the final form of

electrical potential equation in term of water concentration $c_w$ :

$$-\nabla^2\phi = \frac{f}{e-fc_w}\left(\frac{1}{\kappa} - \frac{5}{44}\frac{RTe}{D_wF^2(e-fc_w)^2}\right)(\nabla c_w \cdot \vec{i})$$

$$+\frac{RT}{F}\frac{f}{e-fc_w}\frac{\varepsilon_w^m k_h}{D_w\mu_l}(\nabla c_w \cdot \nabla p_l) \qquad\qquad (6.30)$$

$$-\frac{RT}{F}\left(\frac{f}{e-fc_w}\right)^2(\nabla c_w \cdot \nabla c_w)$$
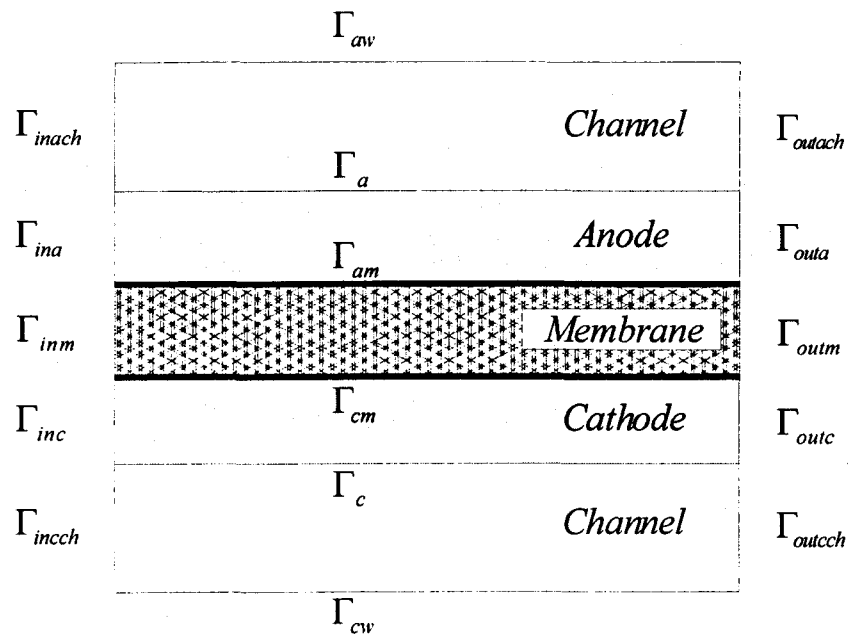
When we switch off the water concentration terms on the right hand side of the above equation, it reduces to *Laplace's* equation, which is commonly used in modeling potential distribution in membrane. Obviously, our newly developed membrane potential equation is more sophisticated than that because of the consideration of water concentration variation in membrane.

# Chapter 7 Boundary Conditions

## 7.1 Modeling Domain and Geometry

Boundary conditions have to be applied at all outer interfaces of the computational domains. Since the present model is coupled with a computational fluid dynamics model, it is convenient to specify boundary conditions by splitting up the entire modeling domain into three sub-domains, *i.e. Main Domain, Water Transport Domain, and Electrical Potential Domain*. A schematic illustration of these domains along with the boundaries and interfaces is given in figure 4.

- The *main domain* accounts for the flow, heat and mass transfer of the reactant gases inside the flow channels and the gas-diffusion electrodes;

- *Water Transport Domain* is used to solve for the flux of liquid water through the membrane-electrode-assembly;

- *Electrical Potential Domain* consists of the membrane only and is used to calculate the electrical potential distribution inside the membrane.

$\Gamma_{av}$

$\Gamma_{inach}$     *Channel*     $\Gamma_{outach}$

$\Gamma_a$

$\Gamma_{ina}$     *Anode*     $\Gamma_{outa}$

$\Gamma_{am}$

$\Gamma_{inm}$     *Membrane*     $\Gamma_{outm}$

$\Gamma_{cm}$

$\Gamma_{inc}$     *Cathode*     $\Gamma_{outc}$

$\Gamma_c$

$\Gamma_{incch}$     *Channel*     $\Gamma_{outcch}$

$\Gamma_{cw}$

(a) Main Domain

$\Gamma_a$

$\Gamma_{ina}$     *Anode*     $\Gamma_{outa}$

$\Gamma_{am}$

$\Gamma_{inm}$     *Membrane*     $\Gamma_{outm}$

$\Gamma_{cm}$

$\Gamma_{inc}$     *Cathode*     $\Gamma_{outc}$

$\Gamma_c$
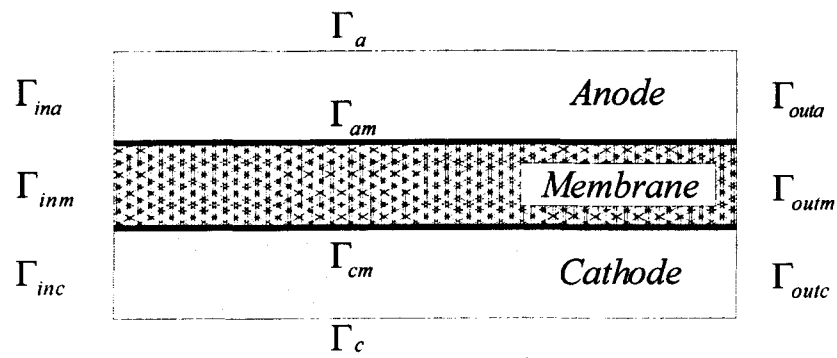
(b) Water Transport Domain (MEA)

$\Gamma_{am}$

$\Gamma_{inm}$     *Membrane*     $\Gamma_{outm}$

$\Gamma_{cm}$
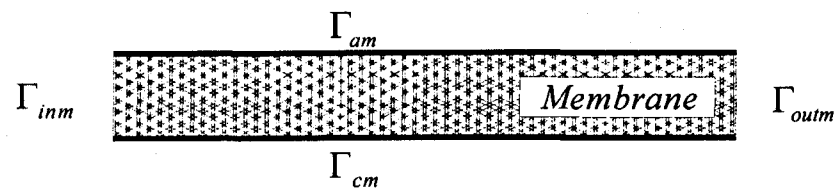
(c) Electrical Potential Domain

Figure 4 Computational domains and boundaries/interfaces

## 7.2 Main Domain

For the *Main Domain*, the environment temperature, $T_{envir}$, and no-slip condition are prescribed on the walls of $\Gamma_{aw}$ and $\Gamma_{cw}$.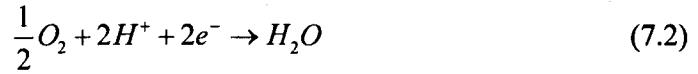 At the two inlets $\Gamma_{inach}$ and $\Gamma_{incch}$, the horizontal inflow velocity, $u$, the environment temperature, $T_{envir}$, and the mass fractions $\omega_{O_2}$, $\omega_{H_2}$ and $\omega_{H_2O_g}$ (*Dirichlet Boundary Conditions*) are needed to be specified.

According to the following two half cell reactions:

$$H_2 \rightarrow 2H^+ + 2e^- \tag{7.1}$$

and

$$\frac{1}{2}O_2 + 2H^+ + 2e^- \rightarrow H_2O \tag{7.2}$$

we can see that a half mole of $H_2$ or a quarter mole of $O_2$ is needed to produce one mole of electrons with the charge of one Coulomb. Then the relationship between the horizontal inflow velocity, $u$, and the stoichiometric flow rate, $\xi$, the desired current density, $i$, can be obtained as follows:

at $\Gamma_{inach}$:

$$u_a = \xi_a \frac{1}{2} \frac{i}{F} \frac{RT_{envir}}{X_{H_2}^{in} P_{g,a}} \tag{7.3}$$

and at $\Gamma_{incch}$

$$u_c = \xi_c \frac{1}{4} \frac{i}{F} \frac{RT_{envir}}{X_{O_2}^{in} p_{g,c}}$$ (7.4)

where $R$ and $F$ denote the gas universal constant (8.3143 J/mol-K) and Faraday constant (96487 Coulomb/mol), respectively.

Then only two different pressure values, $p_{g,a}$ and $p_{g,c}$ representing a pressure drop across the MEA are needed to be prescribed at the two outlet boundaries $\Gamma_{outach}$ and $\Gamma_{outcch}$. Note the slight variation of pressure along each gas flow channel is ignored here. For all other variables, the gradients in the flow direction are assumed to be zero (*Neumann Boundary Conditions*).

At the internal interfaces, *i.e.* $\Gamma_a$ and $\Gamma_c$ on each side, it is not necessary to specify any values, because the gas flow channel model presented in this project will be extended to the neighbouring electrode model with slight modifications by introducing porosity of electrodes and then all the modeling equations will be iteratively solved using a digital computer.

Finally, we should note that the membrane in this domain is simply used as a separator between the anode and the cathode side. It is considered impermeable for the reactant gases. Properties of our interest in the membrane are the liquid water flux and electrical potential, which will be accounted for in the other two domains.

## 7.3 Water Transport Domain

For the liquid water transport through the MEA in this domain, the pressure is given at the interfaces between electrodes and channels, *i.e.* $\Gamma_a$ and $\Gamma_c$:

$$p_{l,a} = p_a \tag{7.5}$$

and

$$p_{l,c} = p_c \tag{7.6}$$

That means the pressure drop from $\Gamma_c$ to $\Gamma_a$ (figure 4) is required to be kept. Note here, the pressure inside the gas flow channels, as has been mentioned before, is assumed constant at these boundaries. We can do so, because preliminary computations indicated that the pressure drop in the flow channels is very small and can indeed be neglected without a loss of accuracy.

For a specific hydration study in membrane, which is described by equation (6.13), we may fix a $c_w$ value along $\Gamma_{am}$ (see figure 4) and prescribing the water content behaviour at $\Gamma_{cm}$ such that the water balance condition described by equations (5.9) and (5.10) is satisfied on a point-by-point basis throughout the length of the membrane.

## 7.4 Electrical Potential Domain

In consistence with the boundary conditions specified for water concentration equation (6.13), the boundary conditions for proton transport equation (6.30) can be prescribed as follows:

A zero electric potential is set at $\Gamma_{am}$ , *i.e.*

$$\phi = 0 \tag{7.7}$$

and at $\Gamma_{cm}$, the following potential gradient can be specified [5]:

$$\nabla \phi = -\frac{1}{\kappa}\left(\vec{i} - Fc_f\vec{U}_l\right) \tag{7.8}$$

where $\kappa$ is the protonic conductivity of the membrane; $\vec{i}$ is the local current density; $F$ is Faraday's constant; $c_f$ is the fixed-charge concentration inside the membrane and $\vec{U}_l$ is the liquid water velocity.

# Chapter 8 Properties and Parameters

The fuel cell model described in the preceding chapters accounts for all basic transport phenomena, so a proper choice of the modeling properties and parameters will make it possible to obtain good agreements with experimental results acquired from a real "fuel cell".

The properties and parameters described in this chapter are taken from the open literature and most of the values are for Nafion 117, unless otherwise stated.

## 8.1 Physical Dimensions and Operational Parameters

Table 1 shows the basic physical dimensions of the PEM fuel cell model. As was mentioned in the previous chapter, straight channels are chosen for the reason of simplicity. In addition, only half of the gas channel length is given and will be taken into account when computing because of the consideration of geometrical symmetry. Since the catalyst layers are simplified as source/sink interfaces, the physical dimensions of them are not necessarily given. The membrane thickness is taken from [5], and it refers to a fully wetted Nafion 117 Membrane.

Table 2 gives the basic operating parameters for our fuel cell model. All these were taken

from Bernardi and Verbrugge [4, 5], who used the experimental data of Ticianelli *et al.* [1] as

their base case. The stoichiometric flow ratio for the experiments was not reported.

| Parameters | Value | Unit |
|---|---|---|
| gas channel length (half) | 0.025 | m |
| Gas channel width | 0.001 | m |
| Gas diffusion electrode thickness | 0.00026 | m |
| Membrane thickness | 0.00023 | m |

Table 1 Physical Dimensions of a PEM fuel cell

| Parameters | Symbol | Value | Unit |
|---|---|---|---|
| Inlet fuel and air temperature | $T$ | 80 | °C |
| Air stoichiometric flow rate | $\xi_c$ | 3.0 | - |
| Fuel stoichiometric flow rate | $\xi_a$ | 1.3 | - |
| Pressure at cathode side | $p_c$ | 5 | atm |
| Pressure at anode side | $p_a$ | 3 | atm |
| Relative humidity of inlet gases | $\alpha$ | 100 | % |
| $O_2/N_2$ volume ratio | $\varepsilon_c$ | 3.76 | - |
| $H_2/CO_2$ volume ratio | $\varepsilon_a$ | 2.56 | - |

Table 2 Operational parameters for a PEM fuel cell under a typical condition

Using equations from previous chapters, some of the boundary conditions, such as the

horizontal velocity components and mass fraction of gaseous species, can be obtained by virtue

of the above operating parameters.

## 8.2 Electrode Parameters and Gas-phase Diffusivities

Electrode properties for a base case study are listed in Table 3. The effective thermal

conductivity $\lambda^{eff}$ has been taken from an expression given by Guran *et al.* [16]:

$$\lambda^{eff} = -2\lambda_{gr} + \cfrac{1}{\cfrac{\gamma_g}{2\lambda_{gr} + \lambda_g} + \cfrac{1-\gamma_g}{3\lambda_{gr}}} \tag{8.1}$$

where the thermal conductivity of the graphite matrix is $\lambda_{gr} = 150.6W / m \cdot K$ and $\gamma_g$ is the

electrode porosity. Since the conductivity of the gases is several orders of magnitude lower, it

can be neglected and the expression above can be simplified to:

$$\lambda^{eff} = \left( \frac{6}{2 + \gamma_g} - 2 \right) \lambda_{gr} \tag{8.2}$$

The reference exchange current density $i_0^{ref}$ is one of the most sensitive parameters in this

model, as it determines the activation overpotential, which is necessary to obtain a certain

current density. This value should be adjusted based on different electrode situation according

to the data available in the open literature.

The experimentally determined binary diffusivities listed in Table 4 can be taken and scaled

for various operating temperature and pressure according to [28]:

$$D_{ij} = D_{ij}^0(T_0, p_0) \frac{p}{p_0} \left( \frac{T}{T_0} \right)^{1.75} \tag{8.3}$$

| Parameters | Symbol | Value | Unit | reference |
|---|---|---|---|---|
| Electrode porosity | $\gamma_g$ | 0.4 | - | [5] |
| Hydraulic permeability | $k_p$ | $4.73 \times 10^{-19}$ | $m^2$ | [5] |
| Effective thermal conductivity | $\lambda$ | 75.3 | W/(m-K) | [16] |
| Transfer coefficient, anode side | $\alpha_a$ | 0.5 | - | - |
| Transfer coefficient, cathode side | $\alpha_c$ | 1 | - | [1] |
| Anode ref. exchange current density | $i_{0,a}^{ref}$ | 0.6 | $A/cm^2$ | [33] |
| Cathode ref. exchange current density | $i_{0,c}^{ref}$ | $4.4 \times 10^{-7}$ | $A/cm^2$ | [1] |
| Hydrogen concentration parameter | $\gamma_{H_2}$ | 0.5 | - | [16] |
| Oxygen concentration parameter | $\gamma_{O_2}$ | 1 | - | [34] |

Table 3 Electrode properties for a PEM fuel cell under a typical condition

| Gas-Pair | Reference Temperature $T^0[K]$ | Binary Diffusivity $D_{ij}^0[cm^2/s]$ |
|---|---|---|
| $D_{H_2-H_2O}$ | 307.1 | 0.915 |
| $D_{H_2-CO_2}$ | 298.0 | 0.646 |
| $D_{H_2O-CO_2}$ | 307.5 | 0.202 |
| $D_{O_2-H_2O}$ | 308.1 | 0.282 |
| $D_{O_2-N_2}$ | 293.2 | 0.220 |
| $D_{H_2O-N_2}$ | 307.5 | 0.256 |

Table 4 Binary diffusivities at 1 atm at reference temperature

In the gas diffusion electrodes, the above binary diffusivities have to be corrected for the porosity. This is often done by applying the so-called *Bruggemann correction* [29]:

$$D_{ij}^{eff} = D_{ij} \times \gamma_g^{1.5} \tag{8.4}$$

where $\gamma_g$ is the electrode porosity.

## 8.3 Membrane Properties

The parameters of our newly developed membrane model are chosen from various open literatures and have their significant characteristics: taking account of the water concentration and temperature variation.

**Conductivity of Membrane**

The conductivity of the membrane is dependent on the water content. When considering the temperature effect, the conductivity, $\kappa$, for the Nafion 117 membrane, can be updated by the following empirical relation [6]:

$$\kappa = (0.5139\lambda - 0.326)\exp\left(1268\left(\frac{1}{303} - \frac{1}{T}\right)\right) \tag{8.5}$$

From chapter 6, we know that the hydration of membrane can be represented by water concentration in membrane, *i.e.* equation (6.10), so we have:

$$\kappa = \left(0.5139\frac{c_w}{e - fc_w} - 0.326\right)\exp\left(1268\left(\frac{1}{303} - \frac{1}{T}\right)\right) \tag{8.6}$$

Then the conductivity in (6.30) should be updated by the new $\kappa$ from the above equation.

**Viscosity of Water**

As a function of temperature, the viscosity of water can be estimated from the empirical relation given by White [30]:

$$\ln\left(\frac{\mu}{\mu_0}\right) = -1.704 - 5.306 \times \frac{273}{T} + 7.003 \times \left(\frac{273}{T}\right)^2 \qquad (8.7)$$

where $\mu_0 = 1.788 \times 10^{-3} \, \text{kg/(m·s)}$. The above formula is valid in the range of $273 \leq T \leq 373K$.

**Volume fraction of water**

Due to the expansion caused by water in membrane, the volume fraction of water $\varepsilon_w^m$ should be treated as a function of hydration. For Nafion 117, we use the expression for $\varepsilon_w^m$ given by [6]:

$$\varepsilon_w^m = 0.35\left(\frac{\lambda}{16.8}\right) \qquad (8.8)$$

note this parameter varies considerably amongst different membranes. The above equation can also be rewritten in term of water concentration as:

$$\varepsilon_w^m = \frac{c_w}{48\left(e - fc_w\right)} \qquad (8.9)$$

where $f$ is an experimentally determined swelling coefficient for the membrane. For Nafion 117 it is given by [6]:

$$f = 0.0126 \tag{8.10}$$

and $e$ is given by equation (6.9):

$$e = \frac{\rho_m^{dry}}{E_m} \tag{8.11}$$

where the dry membrane density, $\rho_m^{dry} = 1980 kg/m^3$, and equivalent membrane weight, $E_m = 1.1 kg/mol$ are reported by Fales *et. al.* [31]. Thus

$$e = \frac{1980}{1.1} = 1800 \quad \text{mol/m}^3 \tag{8.12}$$

**Water Diffusion Coefficient**

C.West and T. F. Fuller have shown that the water diffusion coefficient in a PEM fuel cell can be related to hydration and temperature by the following formula [32]:

$$D_w = 2.5 \times 10^{-7} \lambda \exp(-2436/T) \tag{8.13}$$

or, in term of water concentration:

$$D_w = 2.5 \times 10^{-7} \frac{c_w}{e - f c_w} \exp(-2436/T) \tag{8.14}$$

**Hydraulic and Electric Permeabilities**

The values of hydraulic and electric permeabilities can be found from literature [31] and [5] as:

$$k_h = 1.58 \times 10^{-18} m^2 \tag{8.15}$$

and

$$k_\phi = 7.18 \times 10^{-20} \, m^2 \tag{8.16}$$

# Chapter 9 Conclusions

## 9.1 Summary and Scope

Based on earlier modeling studies, a two-dimensional, non-isothermal and non-isobaric model for a complete PEM fuel cell is developed in this project. Particularly, a new membrane model that takes into account the three main transport mechanisms – diffusion of water, the pressure variation, and the electro-osmotic drag in the membrane, is formulated. The comprehensive model accounts for the fluid flow inside the gas flow channel and porous electrodes, water management, heat and mass transfer, so it is expected to predict the concentration distribution of the reactant gases, the temperature profile and local current densities as well as the fuel cell performance under various operating conditions.

More importantly, we developed an equation describing the electrical potential variation in membrane, which appears more sophisticated than the conventionally adopted fully-saturated-membrane-assumption based *Laplace's* equations since the water content variation in membrane is considered. So, using the newly developed electrical potential equation, the effects of partial hydration in membrane on PEM fuel cell performance are explorable.

The project mainly consists of two parts: an introduction to PEM fuel cell, including its background information, operation principle and components summary is given in the first part, Also, the working principle of PEM fuel cells is introduced from the points of view of chemistry and thermodynamics. In the literature review section, the history of Fuel cell modeling study and some of the latest trends are briefly introduced. In the second part of the project, based on the conservation law for mass, momentum and energy and four phenomenological equations used in previous work, a two-dimensional, non-isothermal and non-isobaric mathematical model for a complete fuel cell is developed. By studying relevant transport phenomena in PEM fuel cell technology, we might expect to predict the velocity, temperature and species distribution in a cell and reveal the relationship between various operational parameters and fuel cell performance. Also, in this part, the boundary conditions for this model, the properties and parameters taken from open literature, including both empirical relations from experimental work as well as the theoretical equations based on different theories are given to complete the whole FEM fuel cell modeling.

In a word, the mathematical model formulated in this project provides a basic framework for PEM fuel cell modeling study and the membrane part of the model demonstrates a sample of modeling expansion according to some empirical natures for a kind of specific membrane, Nafion 117.

## 9.2 Application

The predicting capabilities of the developed model can provide valuable insight and guidance for design, performance optimization and cost reduction of PEM fuel cells.

By solving gas flow channel and electrode model, the concentration distributions of hydrogen and oxygen, which are directly related to the local current distribution, can be obtained. Particularly, at high current density, the concentration overpotential can be detailedly examined based on the concentration distribution analysis at the surface of electrodes. Thus the optimum parameters, such as stoichiometric flow ratio, mass flux of inlet gases, porosity of electrode and pressure gradient can be optimally chosen by performing numerical experiments.

Using our newly developed membrane model, the effects of water content variation on the cell potential across the membrane can be numerically observed. This will provide guidance for determining optimal water content, pressure gradient selection and cooling system design for the whole fuel cell and finally an effective water management scheme can be proposed.

The model can also simulate the effects of various properties and parameters on the cell performance such as the transport properties (*e.g.*, $D_w$, $D_p$ and $n_d$ *etc.*) and structural properties (*e.g.*, $\gamma$, $\varepsilon_w^m$ and membrane thickness *etc.*), in addition to the conditions of temperature and pressure. These results can serve as a guide in the future design and economical production of PEM fuel cells.

## 9.3 Limitations and Recommendations

Since all the equations in our fuel cell model are based on theoretical conservation law or empirical relations, which have been commonly recognized or verified by many researchers, they are expected to be valid even though the model has not been solved and therefore predictions about its validity cannot be made. However, there are also some limitations in this model that prevent it from being broadly used.

Firstly, like most of the other models which address the de-hydration phenomenon, the present model also relies on experimentally determined parameters which pose a limitation to the extent that the model can be used for different types of membranes. Most of the parameters used in the present model are for Nafion 117 and therefore for other membranes the results might not be entirely valid. Efforts should be made to reduce the dependency on empirical relations as they are useful for a particular type of membrane. Of course, the similar analysis and formula derivation can be done based on the ideas presented in this project as long as the empirical data are available.

Secondly, in the electrodes and flow gas channel, all gaseous species are assumed to be ideal gases. In reality, gases are typically assumed to be ideal at temperatures that are considerably in excess of their critical temperature. The critical temperature of water is 374.15°C while PEM fuel cells' typical operating temperature is below 100 °C, therefore at low temperature this assumption becomes questionable.

Pressure profile is considered linear in the membrane because of its unknowable behaviour. This might not be the case in reality and therefore more sophisticated equations based on analytical or empirical analysis are required to effectively eliminate the limitation.

In our present model, the catalyst layers are simplified as interfaces with source/sink terms. Although in practice, the physical and chemical processes in the catalyst layer, which may influent the heat and mass transfer within the whole cell, are extremely complicated, formulating a more sophisticated and detailed catalyst model would be beneficial.

Additionally, the potential loss due to the fact that hydrogen from anode diffuses through the electrolyte, and reaches cathode, where it reacts directly with the oxygen, *i.e.* cross-over

effect, should be taken into account by incorporating the necessary equations to gain more sophisticated numerical experiment result.

Finally, the most important issue is phase-change. Although at elevated temperatures such as 80 °C, the volume of the liquid water is indeed quite small and the results obtained are only weakly affected by neglecting the effect of phase change, the vaporization of liquid water in the electrodes and the rate at which water vapour condenses is of importance for sophisticatedly modeling mass and energy transport. The condensation of water in the electrode will affect the cell temperature profile, and the rate at which water vapour is absorbed into the membrane material will determine the water vapour flux at the catalyst layer boundaries. Depending on the operating conditions, this boundary flux could significantly affect the overall transport of reactant to the catalyst layer and, furthermore, affect the rate of chemical reaction at catalysts. Thus, expanding the existing model to account for phase-change effects should be an important task in enhancing the present model.

# Appendix: A Summary of Modeling Equations

1. Reversible Cell Potential (*Nernst* Equation):

$$E_{rev,T} = E_{rev}^0 - \frac{\Delta \bar{s}^0}{2F}(T - T^0) - \frac{RT}{2F} \ln \frac{a_{H_2O}}{a_{H_2} a_{O_2}^{1/2}}$$ (2.23)

2. Gas Flow Channel Model:

Continuity Equation:

$$\nabla \cdot (\rho_g \vec{U}_g) = 0$$ (3.1)

Momentum Equation:

$$\rho_g (\vec{U}_g \cdot \nabla) u_g = -\frac{\partial p}{\partial x} - \left( \frac{\partial \sigma_{xx}}{\partial x} + \frac{\partial \sigma_{yx}}{\partial y} \right)$$ (3.2)

$$\rho_g (\vec{U}_g \cdot \nabla) v_g = -\frac{\partial p}{\partial x} - \left( \frac{\partial \sigma_{xy}}{\partial x} + \frac{\partial \sigma_{yy}}{\partial y} \right)$$ (3.3)

Energy Equation:

$$-\nabla \cdot (\lambda_g \nabla T_g) + \nabla \cdot (\rho_g \vec{U}_g H) = 0$$ (3.4)

Mass Transfer Equation:

$$-\nabla \cdot (\Gamma_{gi} \nabla \omega_{gi}) + \nabla \cdot (\vec{U}_g \rho_g \omega_{gi}) = 0$$ (3.12)

*Stefan-Maxwell* Equation:

$$\nabla X_{gi} = -\sum_{j=1(j\neq i)}^{3} \frac{X_{gi}X_{gj}}{D_{ij}}(\vec{U}_i - \vec{U}_j) \tag{3.16}$$

3. Electrode Model:

Gaseous Phase:

Continuity Equation:

$$\nabla \cdot (\rho_g \gamma_g \vec{U}_g) = 0 \tag{4.1}$$

*Darcy's* Law:

$$\gamma_g \vec{U}_g = -\frac{k_{g,p}}{\mu_g}\nabla p_g \tag{4.2}$$

Energy Equation:

$$-\nabla \cdot (\lambda_g^{eff}\nabla T_g) + \nabla \cdot (\rho_g \gamma_g \vec{U}_g H) = 0 \tag{4.5}$$

Mass Transfer Equation:

$$-\nabla \cdot (\Gamma_{gi}\gamma_g \nabla \omega_{gi}) + \nabla \cdot (\vec{U}_g \rho_g \gamma_g \omega_{gi}) = 0 \tag{4.6}$$

Liquid Phase:

Continuity Equation:

$$\nabla \cdot (\gamma_l \vec{U}_l) = 0 \tag{4.3}$$

*Darcy's* Law:

$$\gamma_l \vec{U}_l = -\frac{k_{l,p}}{\mu_l}\nabla p_l \tag{4.4}$$

4. Catalyst Layer Model:

Hydrogen Sink:

$$S_{H_2} = -\frac{\nabla \cdot \vec{i}}{2F}M_{H_2} \tag{5.1}$$

Oxygen Sink:
$$S_{O_2} = -\frac{\nabla \cdot \vec{i}}{4F} M_{O_2}$$
(5.2)

Energy Source Term:
$$\dot{q}_r = \frac{\Delta H_r}{4F} i + V_{cell} i$$
(5.8)

Water Source (cathode):
$$S_{H_2O,c} = \nabla \cdot \left(\frac{\vec{i}}{2F} + \vec{N}_{H_2O_g}\right) M_{H_2O}$$
(5.9)

Water Source (anode):
$$S_{H_2O,a} = (\nabla \cdot \vec{N}_{H_2O_g}) M_{H_2O}$$
(5.10)

Reaction Rate (*Bulter-Volmer* equation):

$$i = i_0 \left[ \exp\left(\frac{\alpha_a F}{RT} \eta_{act}\right) - \exp\left(-\frac{\alpha_c F}{RT} \eta_{act}\right) \right]$$
(5.3)

## 5. Membrane Model:

Water Transport Equation:

$$-D_w \nabla^2 c_w - \varepsilon_w^m \frac{k_h}{\mu_l} (\nabla c_w \cdot \nabla p_l) + \frac{5}{44} \frac{e(\nabla c_w \cdot \vec{i})}{F(e - fc_w)^2} = 0$$
(6.13)

Membrane Potential Equation:

$$-\nabla^2 \phi = \frac{f}{e - fc_w} \left( \frac{1}{\kappa} - \frac{5}{44} \frac{RTe}{D_w F^2 (e - fc_w)^2} \right) (\nabla c_w \cdot \vec{i})$$
$$+ \frac{RT}{F} \frac{f}{e - fc_w} \frac{\varepsilon_w^m k_h}{D_w \mu_l} (\nabla c_w \cdot \nabla p_l)$$
(6.30)
$$- \frac{RT}{F} \left( \frac{f}{e - fc_w} \right)^2 (\nabla c_w \cdot \nabla c_w)$$

# Reference

[1]  E. A. Ticianelli, J. G. Beery, and S. Srinivasan. "Methods to Advance Technology of Proton Exchange Membrane Fuel Cells". *J. Electrochem. Soc.*, 135(9): 2209-2214, 1988

[2]  E. A. Ticianelli, J. G. Beery, and S. Srinivasan. "Dependence of Performance of Solid Polymer Electrolyte Fuel Cells with Low Platinum Loading on Morphologic Characteristics of the Electrodes". *J. Electroanal. Chem.*, 251: 275-295, 1988

[3]  Dawn M. Bernardi. "Water Balance Calculations for Solid-Polymer-Electrolyte Fuel Cells". *J. Electrochem. Soc.*, 137 (11): 3344-3345, 1990

[4]  Dawn M. Bernardi and Mark W. Verbrugge. "Mathematical Model of a Gas Diffusion Electrode Bonded to a Polymer Electrolyte". *AIChE Journal*, 37 (8):1151-1163, 1991

[5]  Dawn M. Bernardi and Mark W. Verbrugge. "A Mathematical Model of the Solid-Polymer-Electrolyte Fuel Cell". *J. Electrochem. Soc.*, 139 (9)2477-2491, 1992

[6]  T. E. Springer, T. A. Zawodzinski, and S. Gottesfeld. "Polymer Electrolyte Fuel Cell Model". *J. Electrochem. Soc.*, 138(8): 2334-2342, 1991

[7]  Thomas F. Fuller and John Newman. "Water and Thermal Management in Solid-Polymer-Electrolyte Fuel Cells". *J. Electrochem. Soc.*, 140 (5): 1218-1225, 1993

[8]  T. V. Nguyen and R. E. White. "A Water and Heat Management Model for Proton-Exchange-Membrane Fuel Cells". *J. Electrochem. Soc.*, 140 (8): 2178-2186, 1993

[9]  J. S. Yi and T. V. Nguyen. "An Along-the-Channel Model for Proton Exchange Membrane Fuel Cells". *J. Electrochem. Soc.*, 145(4): 1149-1159, 1998

[10] J. S. Yi and T. V. Nguyen. "Multicomponent Transport in Porous Electrodes of Proton Exchange Membrane Fuel Cells Using the Interdigitated Gas Distributors". *J. Electrochem. Soc.*, 146 (1): 38-45, 1999

[11] T. V. Nguyen. "A Gas Distributor Design for Proton-Exchange-Membrane Fuel Dells". *J. Electrochem. Soc.*, 143 (5): L103-L105, 1996

[12] W. He, J. S. Yi, and T. V. Nguyen. "Two-Phase Flow Model of the Cathode of PEM Fuel Cells Using Interdigitated Flow Fields". *AIChE Journal*, 46 (10): 2053-2064, 2000

[13] Junbom Kim *et al.* "Modeling of Proton Exchange Membrane Fuel Cell Performance with an Empirical Equation". *J. Electrochem. Soc.*, 142 (8): 2670-2674, 1995

[14] S. A. Grot K. T. Weisbrod and N. E. Vanderborgh. "Through-the-Electrode Model of a Proton Exchange Membrane Fuel Cell". *Electrochemical Society Proceedings*, 95-23: 152-166, 1995

[15] M.Woehr, K. Bolwin, W. Schnurnberger, M. Fischer, W. Neubrand, and G. Eigenberger. "Dynamic Modelling and Simulation of a Polymer Membrane Fuel Cell Including Mass Transport Limitations". *Int. J. Hydrogen Energy*, 23 (3): 213-218, 1998

[16] V. Guran, H. Liu and S. Kakac. "Two-Dimensional Model for Proton Exchange Membrane Fuel Cells". *AIChE Journal*, 44 (11): 2410-2422,1998

[17] S. Um, C. Y. Wang and K. S. Chen. "Computational Fluid Dynamics Modeling of Proton Exchange Membrane Fuel Cells". *J. Electrochem. Soc.*, 147 (12): 4485-4493, 2000

[18] Z. H. Wang, C. Y. Wang and K. S. Chen. "Two-Phase Flow and Transport in the Air Cathode of Proton Exchange Membrane Fuel Cell". *J. Power Source*, 94: 40-50,2001

[19] S. Dutta, S. Shimpalee and J. W Van Zee. "Three-Dimensional Numerical Simulation of Straight Channel PEM Fuel Cells". *J. Applied Electrochem.*, 30: 135-146, 2000

[20] J. O'M Bockris and S. Srinivasan. "Fuel Cells: Their Electrochemistry". *McGraw-Hill*, New York, 1969

[21] J. Larminie and A. Dicks. "Fuel Cell Systems Explained". *Wiley*, Chichester, 2000

[22] R. Byron Bird, Warren E. Stewart and Edwin N. Lightfoot. "Transport Phenomena", second edition, *John Wiley & Sons*, 2001

[23] A. J. Bard and L. R. Faulkner. "Electrochemical Methods", *John Wiley & Sons*, 1980

[24] J. S. Newman. "Electrochemical Systems". *Prentice Hall, Englewood Cliffs*, New Jersey, 1991

[25] T. E. Springer, M. Wilson and S. Gottesteld. "Modeling and Experimental Diagnostics in Polymer Electrolyte Fuel Cells". *J. Electrochem. Soc.*, 140 (12), 1993

[26] D.Singh, D. M. Lu and N. Djilali. "A Two-Dimensional Analysis of Mass Transport in Proton Exchange Membrane Fuel Cells". *Int. J. of Enger. Sci.*, 140 (12), 1993

[27] M. W. Verbrugge and R. F. Hill. "Ion and Solvent Transport in Ion-Exchange Memebranes". *J. Electrochem. Soc.*, 140 (5): 1218-1225, 1993

[28] E. L. Cussler. "Diffusion-Mass transfer in Fluid Systems". *Cambridge University Press*, 1984

[29] R. E. De La Rue and C. W. Tobias. "On the Conductivity of Dispersions". *J. Electrochem. Soc.*,106: 827-836, 1959

[30] F. M. White, "Fluid Mechanics (3rd edition)". *McGraw Hill*, NJ, 1994

. [31] J. L. Fales and N. E. Vandeborough. "The Influence of Ionomer Channel Geometry on Ionomer Transport". *Electrochem. Soc. Proceedings*, 86 (13):179-191, 1986

[32] A. C. West and T. T. Fuller. "Influence of Rib Spacing in Proton-Exchange-Membrane Electrode Assemblies". *J. of Applied Electrochem.*, 26: 557-565, 1996

[33] J. T. Wang and R. F. Savinell. "Simulation Studies on the Fuel Electrode of a $H_2$-$O_2$ Polymer Electrolyte Fuel Cell". *Electrochimica Acta*, 37 (15): 2737-2745

[34] A. Parthasarathy, S. Srinivasan, J. A. Appleby, and C. R. Martin. "Pressure Dependence of the Oxygen Reduction Reaction at the Platinum Microelectrode/Nafion Interface: Electrochemical Impedance Spectroscopic Analysis of Oxygen Reduction Kinetics and Mass Transport". *J. Electrochem. Soc.*, 139 (10): 2856-2862, 1992